Marcellus Shale BEG Natural Fracture Project Final Report

Julia F.W. Gale, Stephen E. Laubach, Laura Pommer
Bureau of Economic Geology,
Jon E. Olson, Jon Holder, Kashif Naseem
Department of Petroleum and Geosystems Engineering
The University of Texas at Austin

Objectives

Background

Operators in the Marcellus Shale gas play are aware of the importance of natural fractures and there has been substantial work on the fracture systems in core and outcrop in the large region covered by this play (Eastern Shale Gas Project reports; Evans, 1980, 1994, 1995; Engelder et al. 2009 and references therein; Lash and Engelder, 2005, 2007, 2009). The most common fractures documented by these authors in core and outcrop are subvertical opening-mode fractures that are broadly strike parallel (J1) or cross-fold joints (J2). Evans (1995) also found strike-parallel veins that post-date the J2 set and Lash and Engelder (2005) describe bitumen-filled microcracks developed during catagenesis. Gale and Holder (2010) found in a study of several gas-shales that narrow, sealed, subvertical fractures are typically present in most shale cores. In shale-gas plays that are produced using hydraulic fracturing stimulation these fractures are nevertheless important because of their interaction with hydraulic treatment fractures (Gale et al., 2007). At the scale of hydraulic fracture stimulation, natural fracture patterns and in situ stress can be highly variable, even though a broad tectonic pattern may be consistent over 100s of miles. Thus, site-specific evaluation of the natural fractures and in situ stress is necessary. Open fractures are observed in a few cases in core. Fracture-size scaling, coupled with a fracture-size control over sealing cementation and a subcritical growth mechanism that favors clustering suggests that open fractures are likely to be concentrated in clusters spaced hundreds of feet apart (Gale, 2002; Gale et al., 2007). Our goal for this project is to characterize the fractures and identify the characteristic spatial arrangement of fractures, including potential clusters of large fractures.

Our emphasis is on characterizing, quantifying and modeling fractures that have grown in the subsurface in a chemically reactive environment through a combination of observation at a range of scales, detailed petrographic and microstructural observation of cement fills, and geomechanical modeling (cf Marrett et al., 1999; Gale, 2002; Laubach 1997, 2003; Olson, 2004). Large natural fractures, open or sealed, are typically sparsely sampled in core or image logs. Yet these are the fractures that would have the most effect in augmenting gas flow or influencing the growth of hydraulic fractures. Our approach overcomes the sampling problem by use of fracture size and spatial scaling analysis coupled with geomechanical modeling. That is, we may make predictions about their attributes without sampling them.

Fracture morphology, orientation, spatial organization and cementation were analyzed using datasets from the project well-experiment area in SW Pennsylvania. We added a dataset from a field area to evaluate the use of outcrop fracture data in reservoir

characterization in the Marcellus, thus expanding the relevance of the study beyond the well-experiment area in SW Pennsylvania.

Summary of Results

- In the Marcellus Shale there are two to three sets of subvertical natural fractures: in the quarry exposures near Union Springs, NY, J1 fractures trend 075°, and J2 fractures trend 335°. In the Marcellus reservoir in SW Pennsylvania in the well experiment location for the project there are three trends: NE (which we interpret as J1), NW (which we interpret as J2) and a third set trending ENE. Fractures in outcrop are up to 40 m long and the tallest is at least 3 m high.
- Induced fractures in the reservoir trend NE-SW.
- An analysis of the spatial organization of the calcite-sealed fractures in the Union Springs quarry location we found J1 fractures have a weak preferred spacing at 0.2m, 1 m, ~7 m and 14 m. J2 fractures show preferred spacing at 2, 4 and 14 m.
- J2 fractures in the Gulla Unit #10H horizontal well image log show a preferred spacing at 12.5 m, which is comparable to the vertical distance between limestone beds observed in the nearby Paxton Isaac Unit #7 well. This may be a characteristic mechanical layer thickness, which is reflected somewhat in the fracture spacing.
- Samples from the Paxton Isaac Unit #7 well yield subcritical indices from 38 to 131, with a mean of 75, and fracture toughness, KIc, typically from 1.0 – 1.7 MPa sqrm.
- Geomechanical models using measured and selected input parameters specific to the subsurface close to the Gulla and Paxton Isaac wells yield fracture spacing patterns comparable to those measured directly: geomechanical modeling is a useful predictive tool.
- Horizontal fractures seen in cores were not observed in outcrop.
- The fractures in the outcrop are mostly barren, with the exception of a few examples including those at the Wolfe Quarry in Union Springs.
- Fractures in core are mostly sealed. Barren fractures do occur, but where orientation is known these are parallel to S_{Hmax} and are interpreted as drilling-induced fractures.
- Sealing cements in fractures are calcite, quartz, pyrite, barite and anhydrite. The cement crystals may be sub-euhedral, anhedral or fibrous. Cements commonly show crack-seal texture indicating multiple opening events.
- Larger fractures (> 5 mm wide) may be partly open, with euhedral cement lining open pores: examples were observed in the Onondaga Lst. in the Hardie Unit #1 core, and in the shale facies in other proprietary cores outside this study. Fractures in the shale that are narrower than this are completely sealed, but fractures as narrow as 1 mm have been observed with fracture porosity within a carbonate in the Dunn Clingermann well. There is also some fracture porosity in fractures that are contained within concretions.

- Fluid inclusions are present in some but not all of the fracture cements (hydrocarbon and aqueous). They are typically absent or are too small to observe with a petrographic microscope in the fibrous cements.
- Preliminary O18 and C13 stable isotope data in calcite cements indicates variation in composition of fluids from which cements were precipitated.

Fracture Characterization from Well Data

Project planning

Project strategy and planning for data acquisition were discussed at a meeting at Range Resources, Carbondale, PA on 12/14/2010. The experimental well for the project was confirmed as the Troyer Space Management Unit #10 in Washington County, PA, and preparations were made for data on five nearby wells to be made available.

Slabbed sections of four Range Resources cores housed at TerraTek in Salt Lake City were examined and photographed on 3-4 March 2011. Sampling took place on November 15-16 after further work on the cores by a third party had been completed. The cores are:

Range Resources Paxton Isaac Unit #7	(Washington Co.)
Range Resources Hardie Unit #1	(Greene Co.)
Great Lakes Energy Dunn Clingerman Unit #4	(Washington Co.)
Great Lakes Energy Stewart Nancy Unit #4	(Washington Co.)

The cores are in Washington and Greene Counties in SW Pennsylvania (Fig. 1). They are taken through the target interval for the Troyer well, which had already undergone hydraulic fracturing with microseismic monitoring at the time of core examination. The aim of the core examination is to characterize the natural fracture system in the vicinity of the Troyer well in order to better understand the behavior of hydraulic fracture treatments, and the permeability system of the Marcellus Shale. A horizontal image log from a fifth well, the Gulla Unit # 10H, in Washington County was provided for fracture orientation and spatial organization analysis.

Sampling of Cores

In November 2011 the cores were sampled for fracture cements, non-cemented fracture surfaces and for subcritical index and tensile strength of fracture planes testing. We used the observations of the archived half of the core, as described above and in the Terratek reports, to select depths from the sampling halves. The sampling inventory is provided in Appendix B.

Additional cores samples were obtained by Edgar Pinzon (GTI) from the Eastern Shale Gas Project #5 (Connie Sokovitz #1) well in Lawrence Co., PA (received at the Bureau facility on June 15th). These samples were collected for subcritical crack index work. The well is located more than 60 miles north of the focus area for the project so the results cannot be used for modeling of the fracture system in the vicinity of the well experiment. Test results would, however, be used to constrain the variability of subcritical index in the Marcellus. Pinzon (pers. comm.) did not observe natural fractures in the cores from

which the samples came. The cores were full diameter, however, and the outer surfaces were rough, which may have obscured any hairline fractures present.

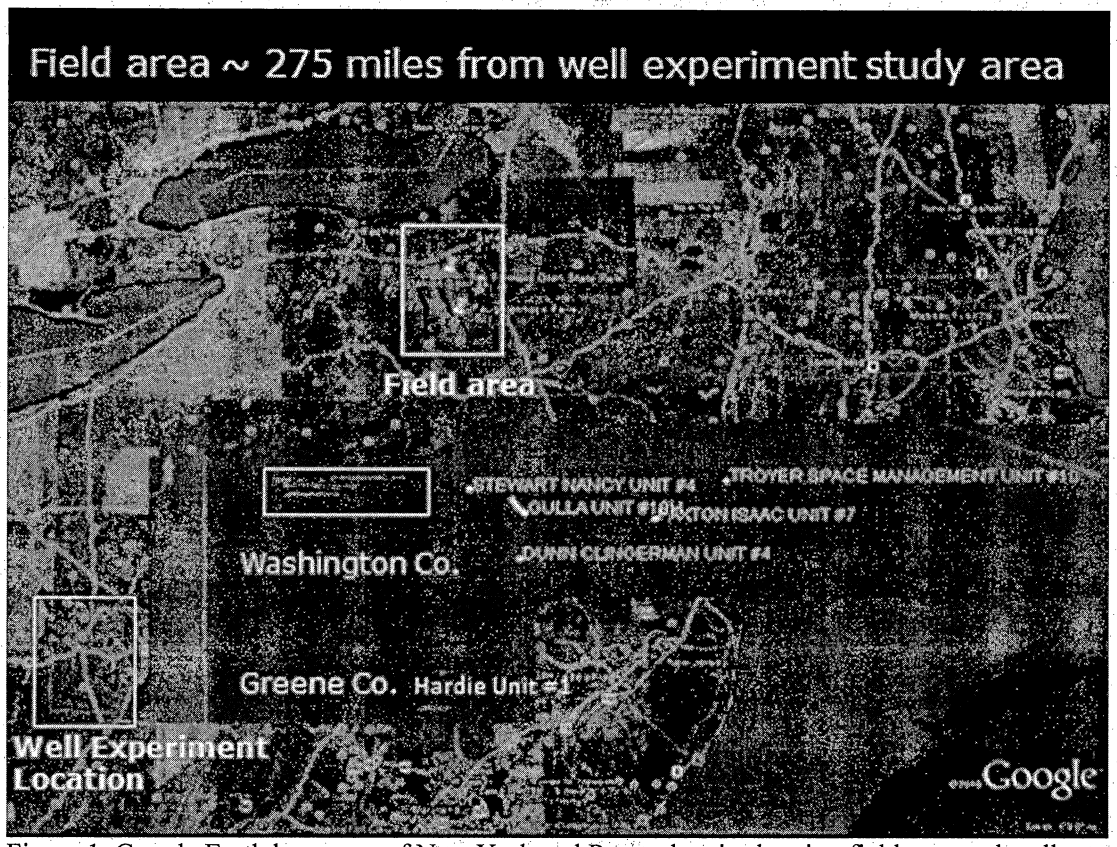

Figure 1. Google Earth base map of New York and Pennsylvania showing field area and well experiment location. Green boxes are enlargements of the well experiment location.

Fracture Characterization and Fracture Cement Petrography

Fracture characterization had already been completed by TerraTek for the two cores that were oriented using scribing techniques: the Paxton Isaac Unit #7 and Hardie Unit #1 cores. The fracture orientations obtained from the core had been calibrated with image logs. Our aim was to augment, not repeat, this work. We used the existing fracture reports to establish that most of the fractures in the whole core are represented in the slabbed viewing half. During the March 2011 visit we photographed the fractures in the slabbed viewing half of these cores and examined the TerraTek fracture description reports provided by Range. We concur with the overall findings of these reports in terms of fracture types. There are some differences in our interpretation of features on a fracture-by-fracture basis and these discrepancies are discussed below.

Fracture descriptions were made of the two unoriented cores (Dunn Clingerman Unit #4; Stewart Nancy Unit #4) as this had not previously been done. These data are included in Appendix A.

The main fracture types described from the cores were sampled and fracture cements observed in thin section using conventional petrography and cold-cathode CL. Calcite is the dominant fracture cement, with quartz, pyrite, barite and anhydrite also present in some fractures. Cements may be fibrous or anhedral-blocky. Characteristic cement types and morphologies are summarized in the photo-panels and captions that follow each fracture core description section.

Range Resources Paxton Isaac Unit #7

This core extends through the entire interval of interest from 5,849 ft in the Rhinestreet Fm. to 6,533 ft in the Onondaga Lst. Fracture types include (1) networks in carbonate concretions, (2) tall, narrow, steeply-dipping, sealed fractures, (3) bedding –parallel sealed fractures (4) shallow-angle faults and (5) drilling-induced fractures. These are described below. The orientations of natural and induced fractures presented in the TerraTek reports are interpreted in relation to the J1/J2 terminology established for the Appalachian basin shales by Engelder and other workers (see Engelder et al., 2009 and references therein) (Fig. 2).

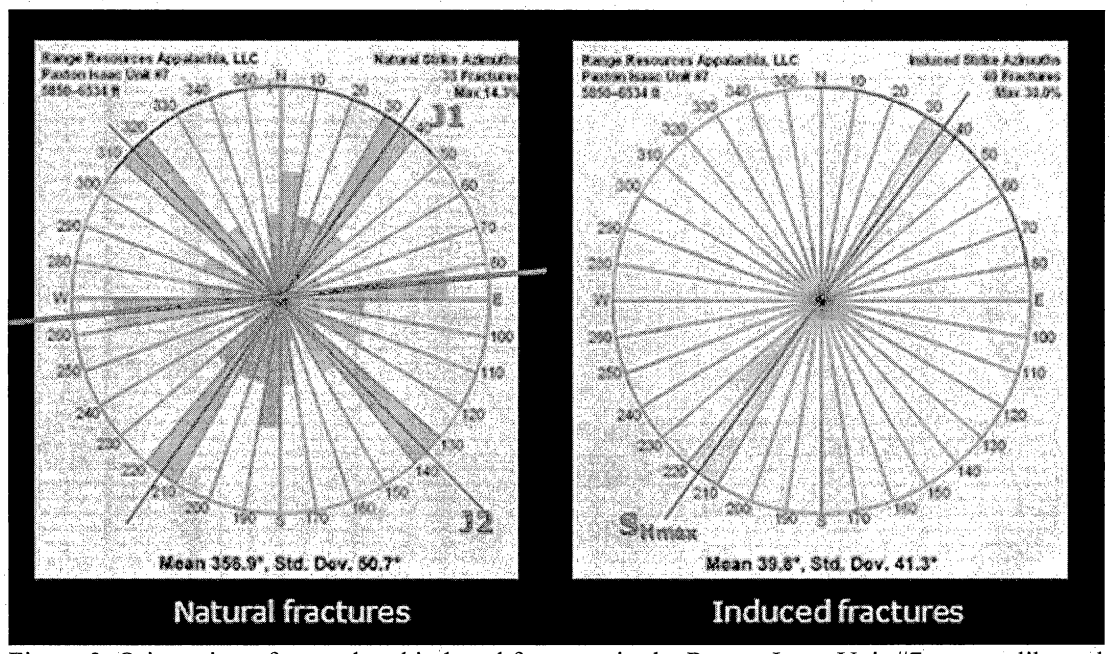

Figure 2. Orientation of natural and induced fractures in the Paxton Isaac Unit #7 core, calibrated by image log. Data collected by TerraTek, red interpretation lines by Gale, this study.

Complex networks that are contained within carbonate concretions (Fig. 3a). While these fractures are unlikely to contribute significantly to reservoir permeability, the cements in the fractures may offer insights into fluid processes operating some time after concretions were established. The concretions themselves might affect propagation of hydraulic fractures.

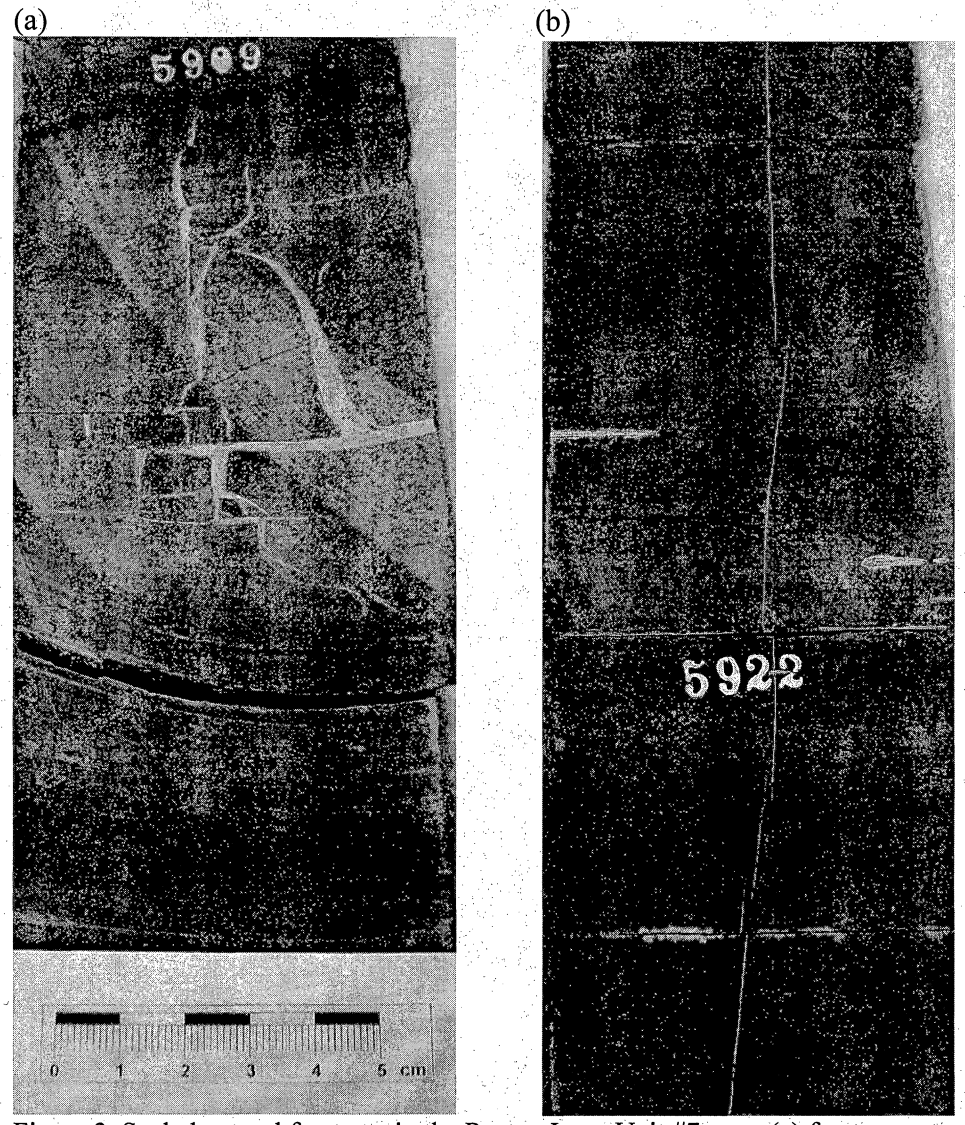

Figure 3. Sealed natural fractures in the Paxton Isaac Unit #7 core, (a) fracture network contained within carbonate concretion (b) tall, segmented steep fractures. Sealing cement is calcite.

Tall (up to 4 ft), steep (dip > 70°), sealed fractures are common in this and the other cores examined (Fig. 3b). These are similar to the fractures described by Gale *et al.*, (2007) in the Barnett Shale, and are interpreted to be part of a fracture population that has a power –law or exponential size distribution. The fractures observed here likely represent the smaller size fraction of the wider population. In some parts of the core (e.g. 6,916 ft) fractures of this type are parallel to the slabbed face and are easily missed.

(a) (b)

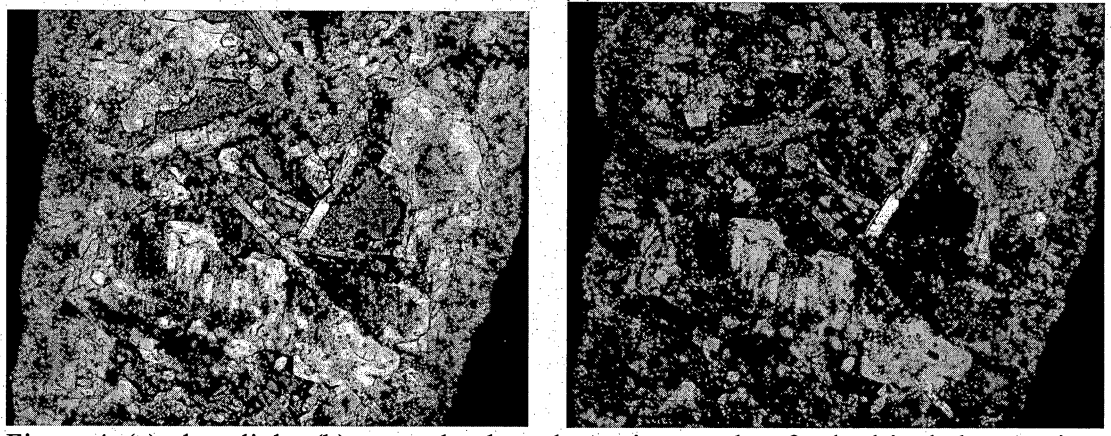

Figure 4. (a) plane light, (b) crossed polars photomicrographs of anhydrite laths growing in fracture pore space. The fracture walls are calcite. This fracture is contained inside a carbonate concretion (Fig. 3a); fracture inside concretions commonly show a different cement pattern and morphology from the fractures cutting the shale. Sample from 5909 ft.

(a) (b)

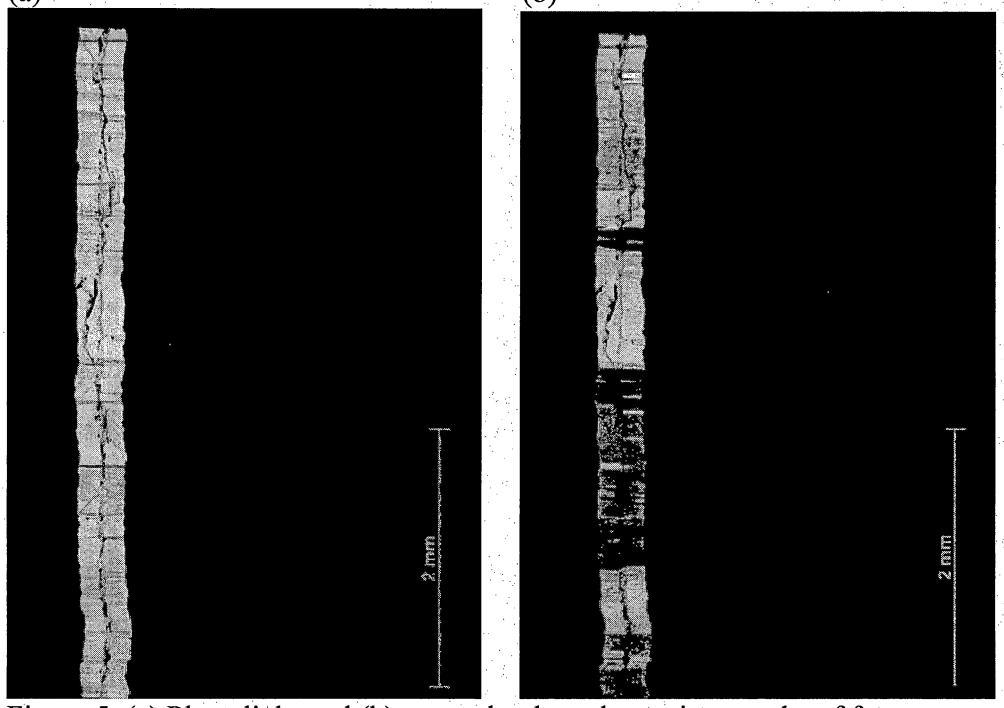

Figure 5. (a) Plane light and (b) crossed polars photomicrographs of fracture cement in a subvertical fracture similar to the example in Fig. 3b. The cement is fibrous calcite with a median line. Adjacent fibers have a common crystallographic orientation so that blocks of fibers move into extinction together (b). Fibres are normal to fracture walls in this case indicating no shear component to the opening. Sample depth 6,231.5 ft.

Bedding-parallel fractures constitute a third fracture type. They are commonly sealed with fibrous calcite (Fig. 6a, b) but others contain blocky calcite cement. These fractures are not common in the core but several are observed together between 6,483 and 6,485 ft in the organic-rich part of the Marcellus Fm. (Fig. 7a). We speculate that these fractures may be associated with fluid overpressure during catagenesis (c.f. Lash and Engelder, 2005) although we did not observe hydrocarbon fluid inclusions in the fibrous cements in this well. Single phase oil inclusions were noted in a horizontal fracture in the Dunn Clingermann well (see section on this well below). In addition to the planar bedding-parallel fractures there are networks of shallow angle, non-planar fractures that may have slickensides along the surfaces and where the host rock is brecciated (Fig. 7b). These are interpreted as zones of shear. In an example at 6,488.2 ft a pyrite-rich layer has been displaced by approximately 2 mm of reverse shear along a shallow-angle fault (Fig. 7c).

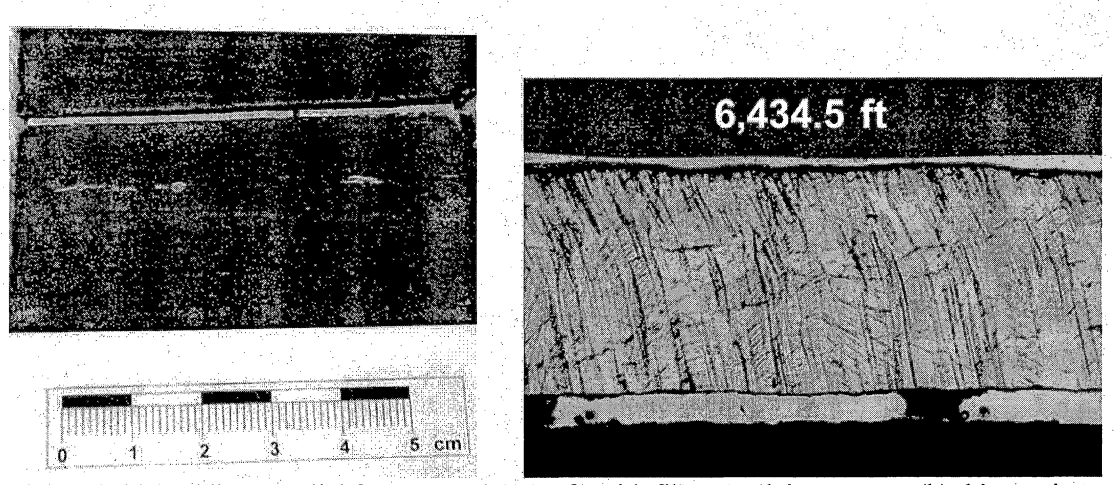

Figure 6. (a) Bedding-parallel fracture at 6,434.5 ft, with fibrous calcite cement. (b) thin section of fracture in (a). Curved fibers indicate a minor horizontal shear component in addition to opening normal to the fracture wall. Oxygen and carbon stable isotopes were analyzed for this sample.

(a) (b)

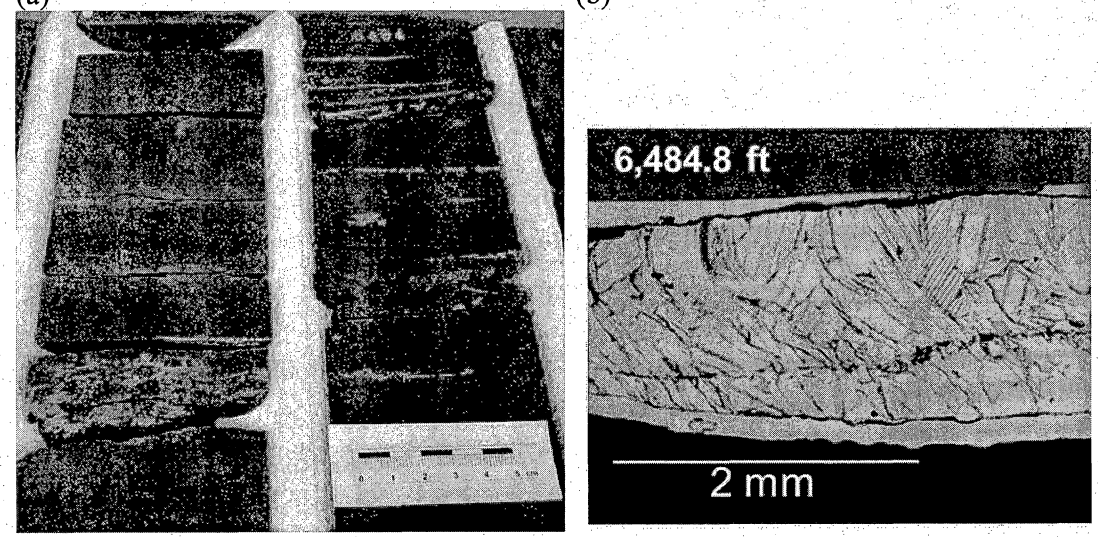

(c) (d)

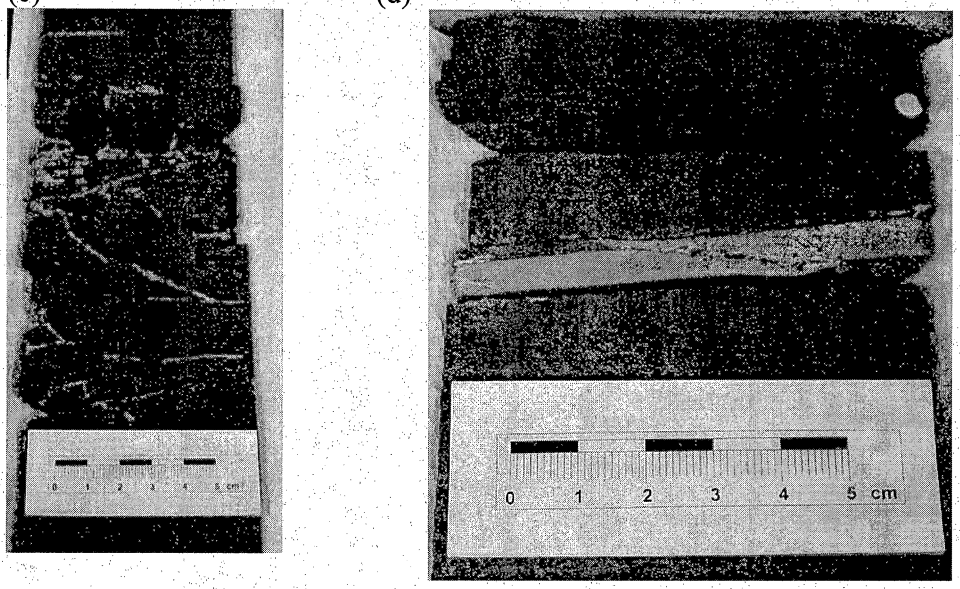

Figure 7. (a) Bedding parallel opening-mode fractures, (b) Plane light photomicrograph of fracture cement in a fracture from bedding parallel fracture in the (Fig. 7a). Curved fibers indicate a minor horizontal shear component in addition to opening normal to the fracture wall. Oxygen and carbon stable isotopes were analyzed for this samples, (c) low angle shears in the Paxton Isaac well, (d) low angle shear cutting a pyrite layer at 6,488.2 ft.

Range Resources Hardie Unit #1

Fracture types present in the Paxton Issac Unit #7 were also observed in the Hardie Unit #1. In addition, there are examples of long fractures originally interpreted as induced, petal centerline fractures (Fig. 8a, b). We reinterpret these fractures as being reactivated natural fractures on the basis of two factors: 1) the dips of the fractures are not subvertical but approximately 70°; they are not truly 'centerline', although the fractures do curve at the upper terminus and have a 'petal' geometry. 2) There are hairline sealed natural fractures in apparently the same orientation in adjacent parts of the core (Fig. 8c, d). In any case it is likely that the strike of these fractures is close to both the paleo- and present day S_{Hmax}.

There are several examples of fractures within carbonate or pyrite concretions that contain a several phases of cement (Fig. 9). We will sample these. While these fractures may not provide conduits for hydrocarbons the cements may reveal information about the fluids and temperature conditions in the basin. The concretions can preserve the pre-compaction state of the shale (Fig. 10).

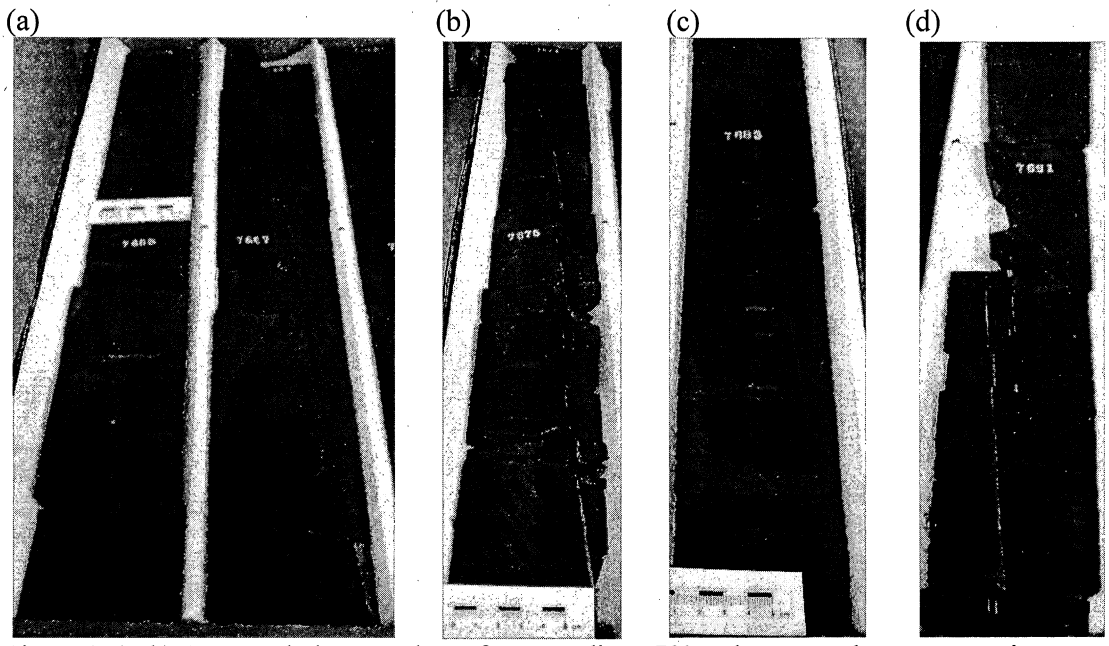

Figure 8. (a, b) Apparently barren, planar fractures dip at 70° and curve at the upper terminus with a 'petal' geometry. These had been interpreted as induced petal centerline fractures. Depths 7,664-7,668 ft and 7,674 ft (c, d) Natural fractures sealed with calcite with similar orientation in adjacent sections of core. Depths 7,683 and 7,691 ft. Hardie Unit #1 core.

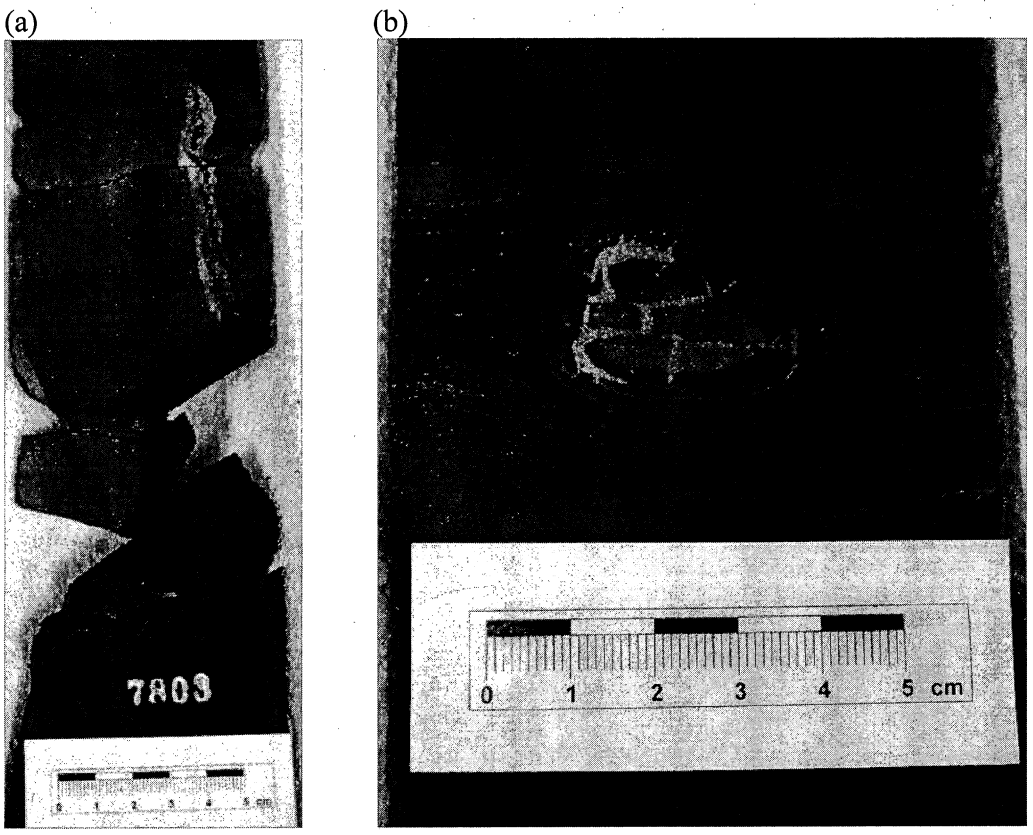

(c)

Figure 9. Fractured carbonate/pyrite concretions with multiple phases of fracture sealing cement, Hardie Unit #1 core. Samples from (a) 7,803 ft and (b) 7,817.5 ft. (c) Plane light photomicrograph of anhydrite, calcite and pyrite cements in the fracture in (a). These are similar to the fractures in the Paxton Isaac well concretions.

Figure 10. Fossils are preserved with their original geometry within a carbonate concretion, but are compacted in the surrounding layers. This is evidence that the concretions grew before compaction of the sediment was complete. Hardie Unit #1 core, 7,847 ft.

In addition to the steep planar fractures with large height to width aspect ratios (Fig. 3b, 8) there are fractures with much lower aspect ratios that occur in en echelon arrays at 7,881 to 7,883 ft (Fig. 11). These are sealed with fibrous carbonate cement. The relationship between these two groups is not known.

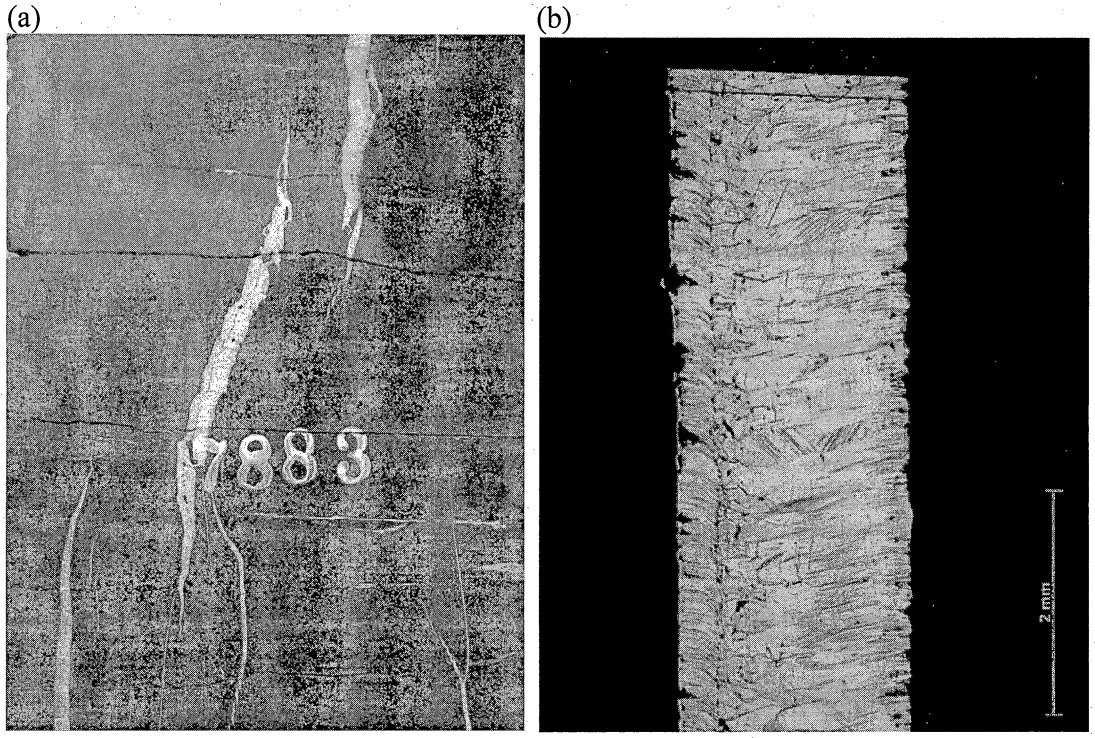

Figure 11. (a) En echelon arrays of low height to width aspect ratios. (b) Thin section photomicrograph showing fibrous calcite fracture fill with variable fiber width and orientation.

The en echelon arrays may also contain complex branching structures near the tips of each segment (Fig. 11a). In other cases fractures may be dominantly vertical but have horizontal (bedding parallel) offshoots (Fig. 12).

Complex branching low angle fractures are also present (Fig. 13; c.f. Fig. 7). Some are bedding-parallel, opening-mode fractures with either blocky or fibrous fill (top of figure). Others have shear offsets and slickensides along them (center of figure).

The unit below the Marcellus, the Onondaga Limestone contains en echelon fractures with vuggy openings in calcite cement (Fig. 14).

(a)

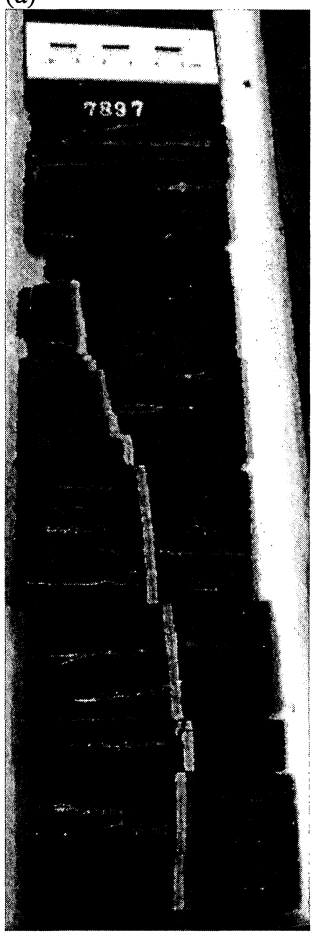

Figure 12 (a) Vertical fracture with fibrous calcite fill and horizontal component at the top break. (b) Both fractures have detached from the fracture walls, and possibly from each other in thin section. Both show curved fibers, which are consistent with contemporaneous opening. The vertical fracture has a median line consistent with growth from the center outwards (antitaxial) whereas the horizontal fracture does not, and has the widest crystals in the center, which is consistent with syntaxial growth from the walls inwards. Sample depth 7897.5 ft.

(b)

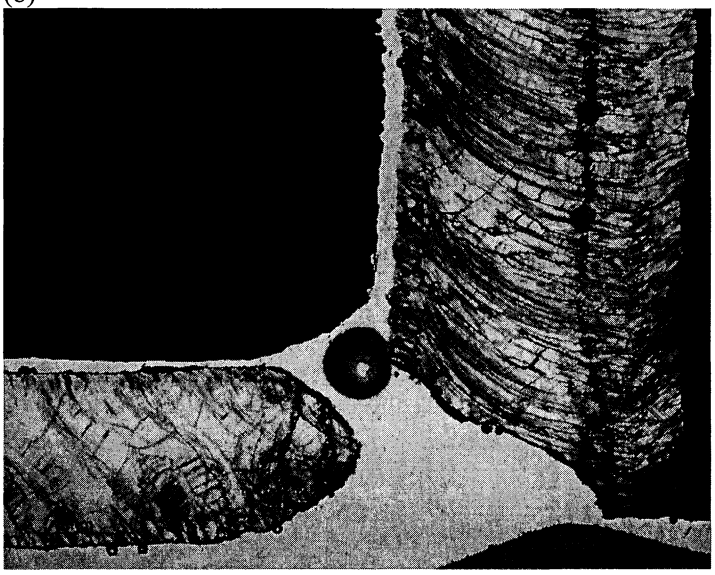

(a)

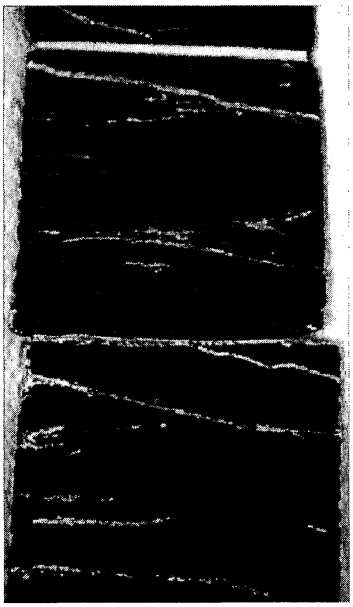

(b)

Figure 13. (a) Low-angle fractures in the Hardie Unit #1 core, 7,889.5 ft. (b) morphologies of these fractures can be irregular, with fracture walls being non-planar.

(a) (b)

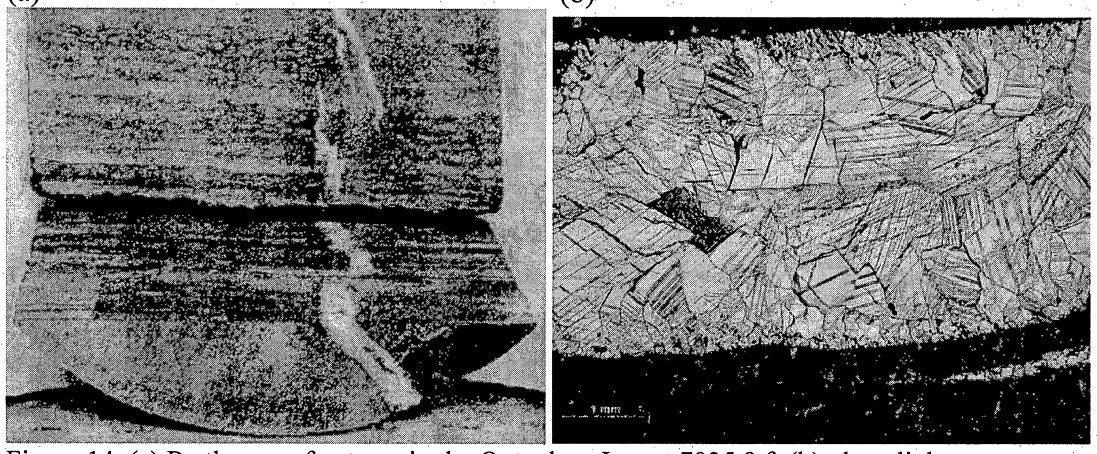

Figure 14. (a) Partly open fractures in the Onondaga Lst. at 7935.8 ft (b) plane light photomicrograph of fracture porosity (blue epoxy) in calcite cement in the sample in (a).

Great Lakes Energy Dunn Clingerman Unit #4

This core is unoriented and a systematic fracture description had not been done previously. We present a spreadsheet showing some of the measurable parameters and descriptive characterization (Appendix A). Here, we present a summary of the findings. As for the other cores described in this report, there are both drilling induced and natural fractures present. We first give examples of fractures similar to those found in the two oriented cores.

Steeply dipping fractures sealed with calcite in the shale section (Fig. 15a), but partly open in the underlying limestone section (Fig. 15b), sealed horizontal fractures, sometimes associated with pyrite (Fig. 16) and low angle fractures (Fig. 17) are present at several locations in this core.

Also present are steep barren fractures (e.g. 6,515.5 to 6,521 ft) that we interpret as drilling induced fractures.

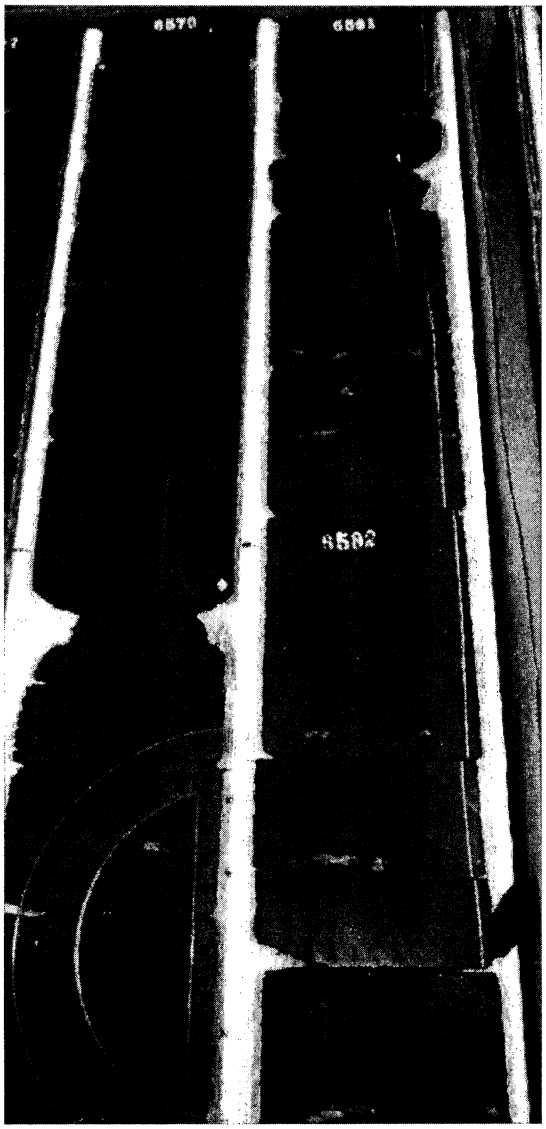

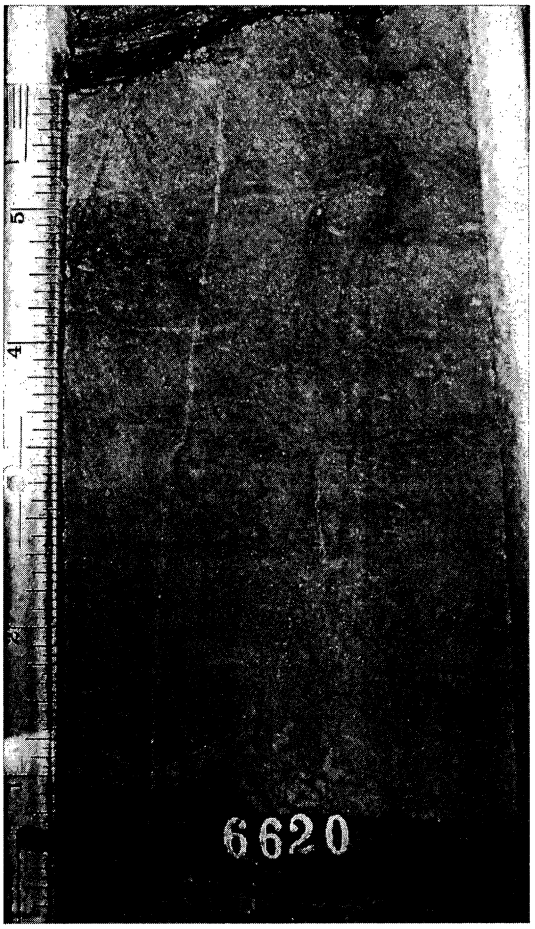

Figure 15. (a) Vertical calcite-sealed fractures at 6,579 to 6,583ft in mudrock, and partly open at 6,620 ft in limestone. We do not know if the fracture sets are the same.

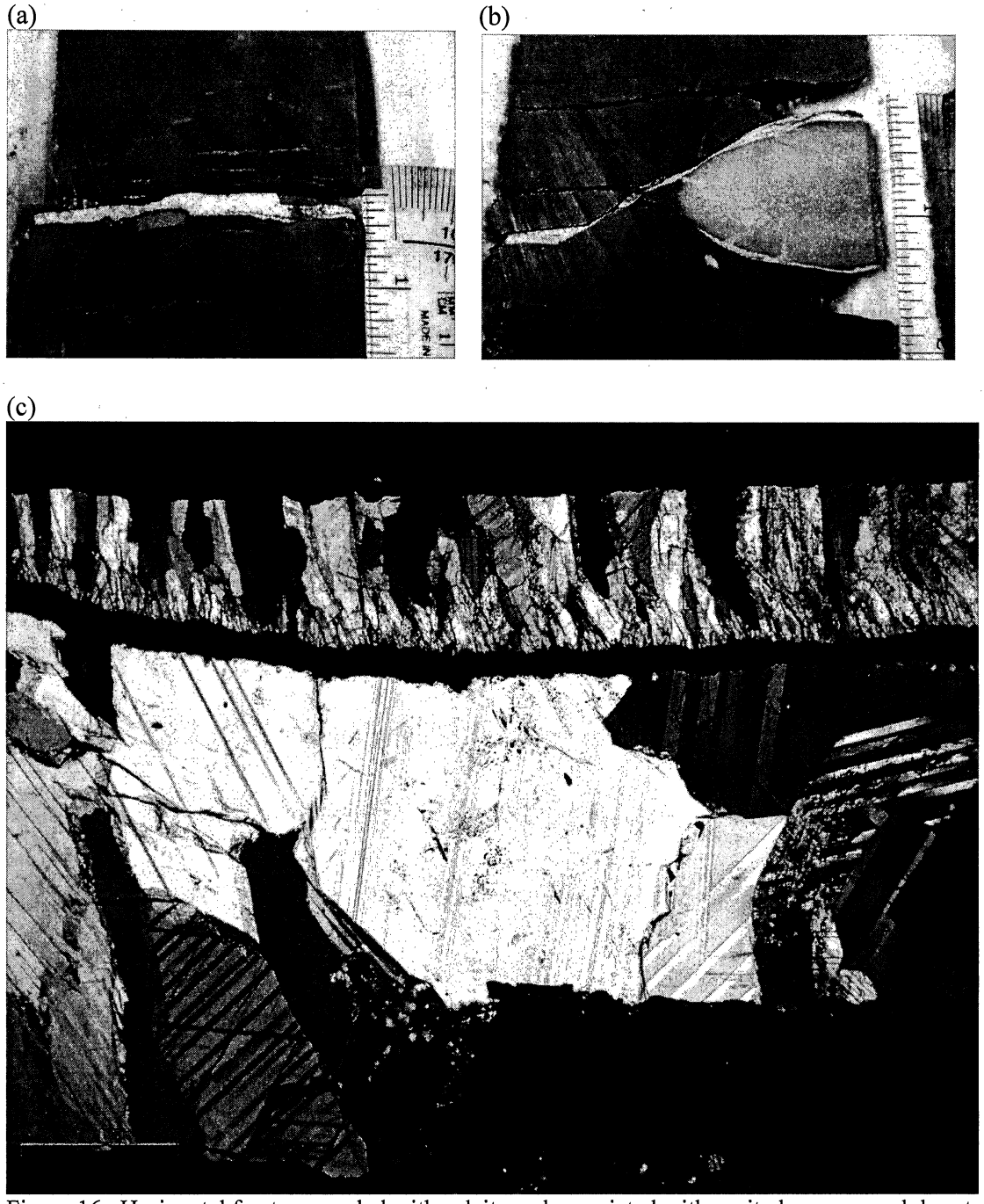

Figure 16. Horizontal fractures sealed with calcite and associated with pyrite layers or nodules at (a) 6,507.6 ft and (b) 6,570.4 ft (c) crossed polars photomicrograph of calcite cement in the fracture in (a). Two different calcite morphologies are present; a coarse blocky cement at the base and a fibrous layer at the top.

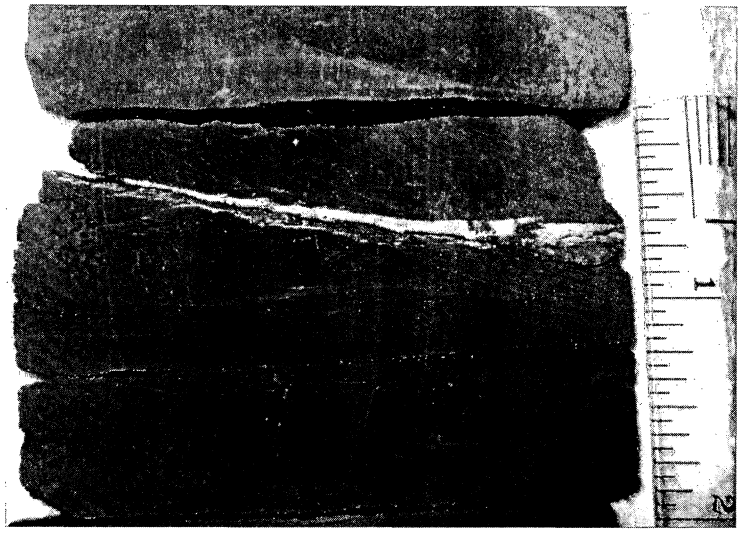

Figure 17. Low angle fracture at 6,567.6 ft.

There are many locations in all wells where there are horizontal accumulations of pyrite. In the Paxton Isaac Unit #7 well there are several of these near the top of the cored interval. Terratek had interpreted these as fractures (Fig. 18a) and many of them are notably crenulate.

(a) (b)

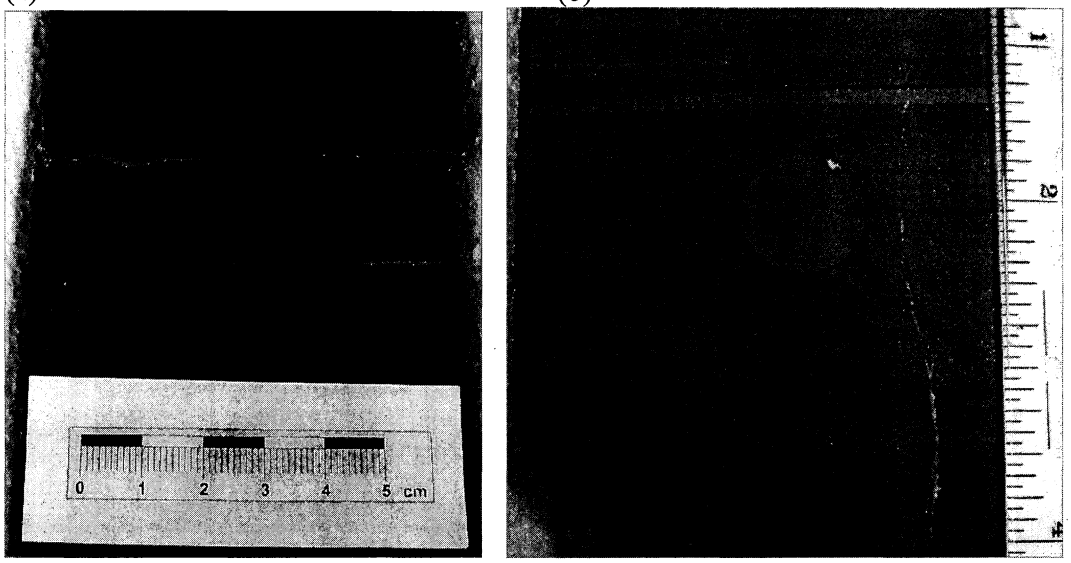

Figure 18. (a) Horizontal accumulations of pyrite of uncertain origin in the Paxton Isaac Unit #7 core at 5,882 ft. (b) Vertical, pyrite-filled fracture in the Dunn Clingerman Unit #4 core at 6,600.5 ft.

We consider that they are not fractures but are likely sedimentary or diagenetic in origin, with the crenulate forms possibly being pyrite replacement of fossils. However, in the Dunn Clingerman well there are vertical, pyrite–filled fractures (Fig. 18b). The origin of the pyrite accumulations is therefore unresolved, but we suspect there is more than one mechanism.

In the crinoidal limestone at the base of the core there are subvertical stylolites, which must be tectonic in origin. We have not established the relationship between the stylolites and the fractures in the limestone. Tectonic stylolites at a high angle to J2 fractures are observed in outcrop in the Tully Limestone in the river section below Taughannock Falls, NY. Engelder and Engelder (1977) described the strain recorded in fossils, including crinoids, and due to solution cleavage in the Appalachian Plateau, concluding that horizontal shortening was of the order of 10%.

Great Lakes Energy Stewart Nancy Unit #4

This core is unoriented and a systematic fracture description had not been done previously. We present a spreadsheet showing some of the measurable parameters and descriptive characterization (Appendix B). This core is notably more disked (many horizontal breaks) than the other cores, which may reflect its composition. There are several accumulations of silt and pyrite that can superficially resemble horizontal fractures (Fig.19). There are very few natural fractures in the core, however, most being concentrated in the lowest 4 ft, where there are sealed fractures associated with concretions and a few calcite-sealed subvertical fractures (Fig. 20).

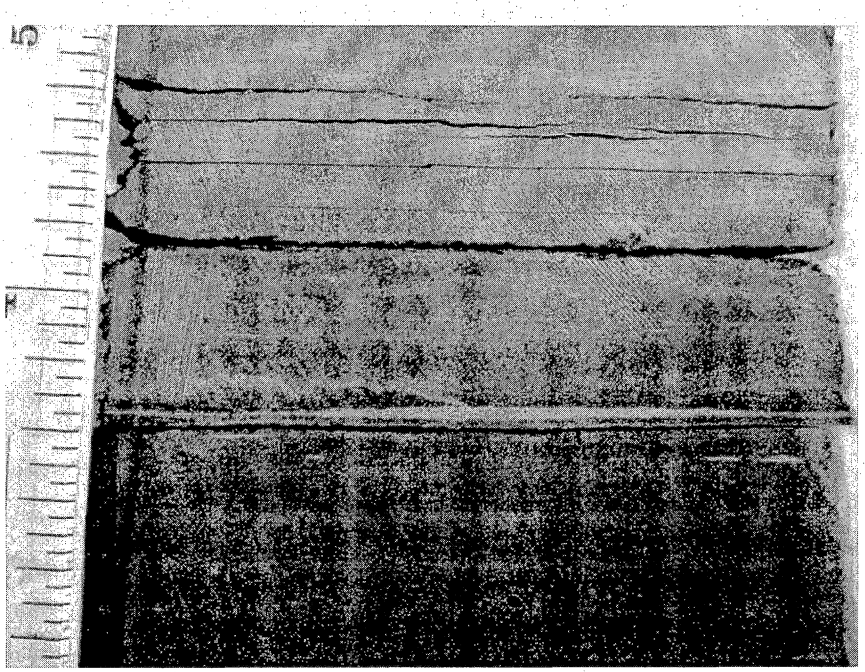

Figure 19. Silt (center) and pyrite (top) accumulations at 6,279.2 ft.

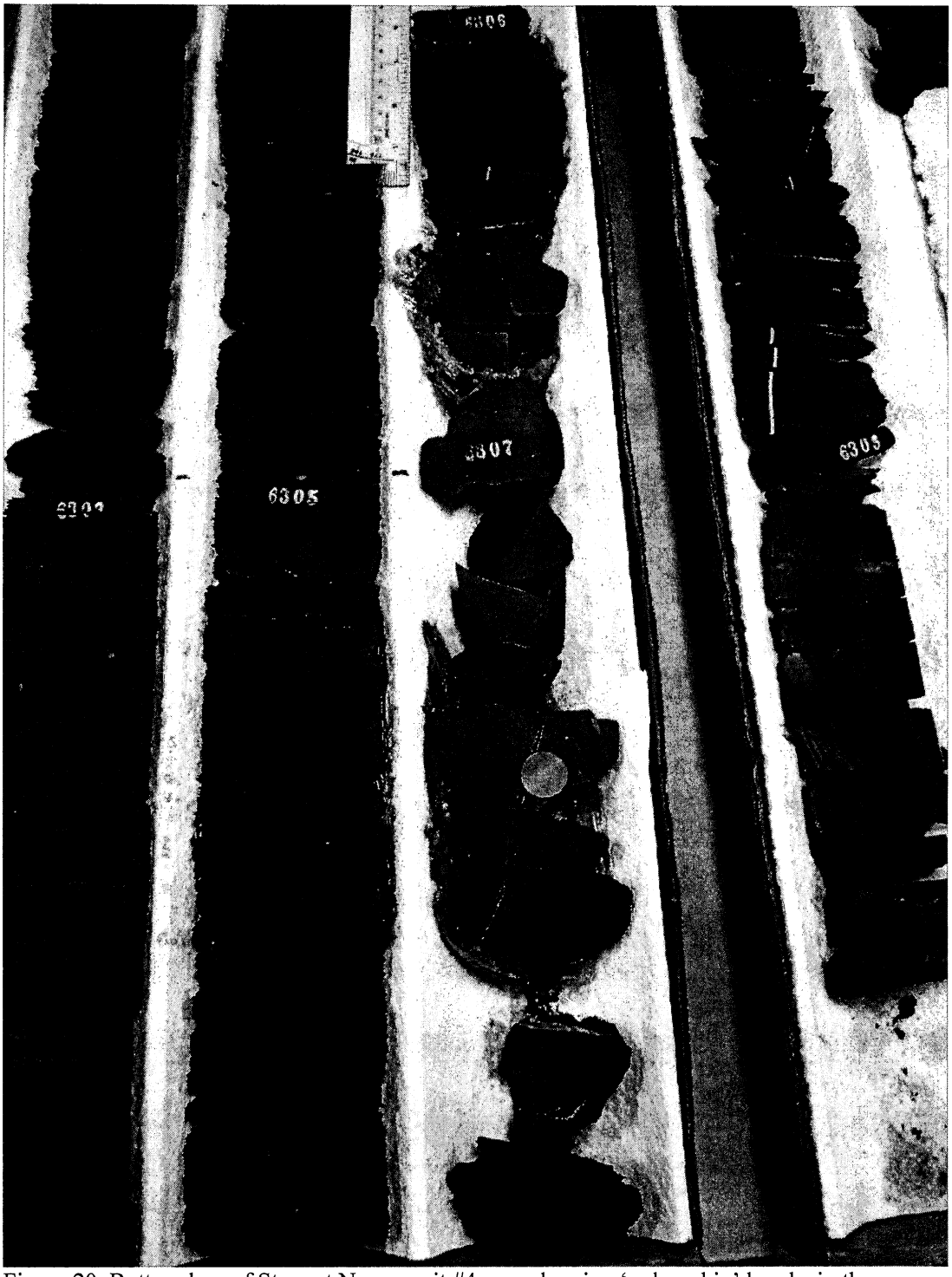

Figure 20. Bottom box of Stewart Nancy unit #4 core showing 'poker chip' breaks in the mudrock interval. A fracture network sealed with calcite and pyrite occurs in the paler grey carbonate concretion and vertical, calcite-sealed fractures are present at the base (6,302 to 6,310 ft).

Additional work

A Petra project was constructed by Laura Pommer (Graduate Research Student, BEG) and Edgar Pinzon (GTI) so that intervals of interest relative to the Troyer Space Management Unit #10 could be identified (Fig. 22). Tops identified on the cores and well log analysis were used to construct tops on the different members in the section and correlate from well to well. The Hardie well depths are greater than those in Washington County. In addition to the target zone for the well itself, units above and below are of interest as they are likely to be reached by the hydraulic fracture treatment.

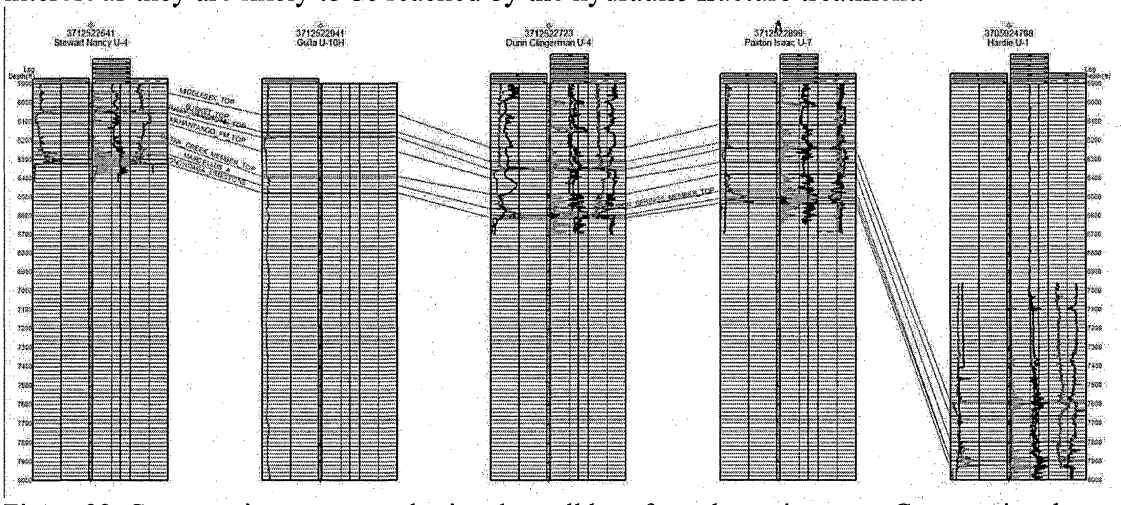

Figure 22. Cross-section constructed using the well logs from the project area. Construction done using Petra.

Field Work

Two field trips occurred during the first year of the project. Dr. Terry Engelder (Pennsylvania State University) led a field trip to several outcrop locations in central Pennsylvania and the Finger Lakes district of New York State on June 2-3, 2011 (Fig. 23). The purpose of the trip was to examine the fracture expression in outcrop in the Marcellus and overlying shale-bearing sequences in the region, and to discuss the overall gas-plume model for natural hydraulic fracturing that Engelder has developed. For this project there were two additional objectives:

1) To compare findings in outcrop with the fracture characterization previously reported for cores from Washington and Greene Counties, SW Pennsylvania in the project focus area. We also viewed two cores at the Penn. State Geology Department core laboratory for comparison.

2) To assess whether additional fieldwork would be beneficial for the project.

As a result of the first trip a data-acquisition trip took place during September 29-31, 2011. The outcrop fracture patterns in the Marcellus Shale have been the subject of many studies over several decades. This second trip was aimed at addressing questions that have not previously been answered. Namely, the apparent anomaly in the number of fractures observed with cement in the subsurface in cores (many) vs. the number of fractures observed with cement in outcrop (few). A further anomaly is that many fractures in core dip at around 70-75°, whereas the joints in outcrop are mostly subvertical (where bedding is horizontal). The only exception observed is one cluster of steeply dipping (~ 70°) J2 fractures adjacent to subvertical ones in Fillmore Glen State Park.

Work by Engelder (2009) suggests that joint sets visible in outcrop represent those in the subsurface as seen in core and borehole image logs. The joints, in both outcrop and subsurface, are observed to be in two main orientations and are hypothesized to have formed "close to peak burial depth as natural hydraulic fractures induced by abnormal fluid pressures generated during thermal maturation of organic matter" (Engelder et al., 2009). If this is correct then outcrop and quarry observations in the Marcellus Shale can thus be used as a proxy for subsurface joint orientation and fracture modeling, as the fractures are essentially "fossil reservoir fractures" (Fidler Thesis, 2011). We collected samples of cement from both fracture sets with the aim of determining whether the cements indeed indicate fracturing occurred at depths (temperatures and pressures) equivalent to the present day Marcellus reservoir. Analysis of these samples is ongoing as part of Pommer's thesis, results of which will be available upon completion. We will compare results with Evans (1995) who found progressively mature hydrocarbon fluid inclusions in fracture cements from fractures of decreasing age in Devonian shales from the Appalachian Basin, relative timing having been established through cross-cutting and abutting relationship. Evans (1995) related these findings using a burial history curve such that the latest fractures developed at peak burial for the Devonian shales.

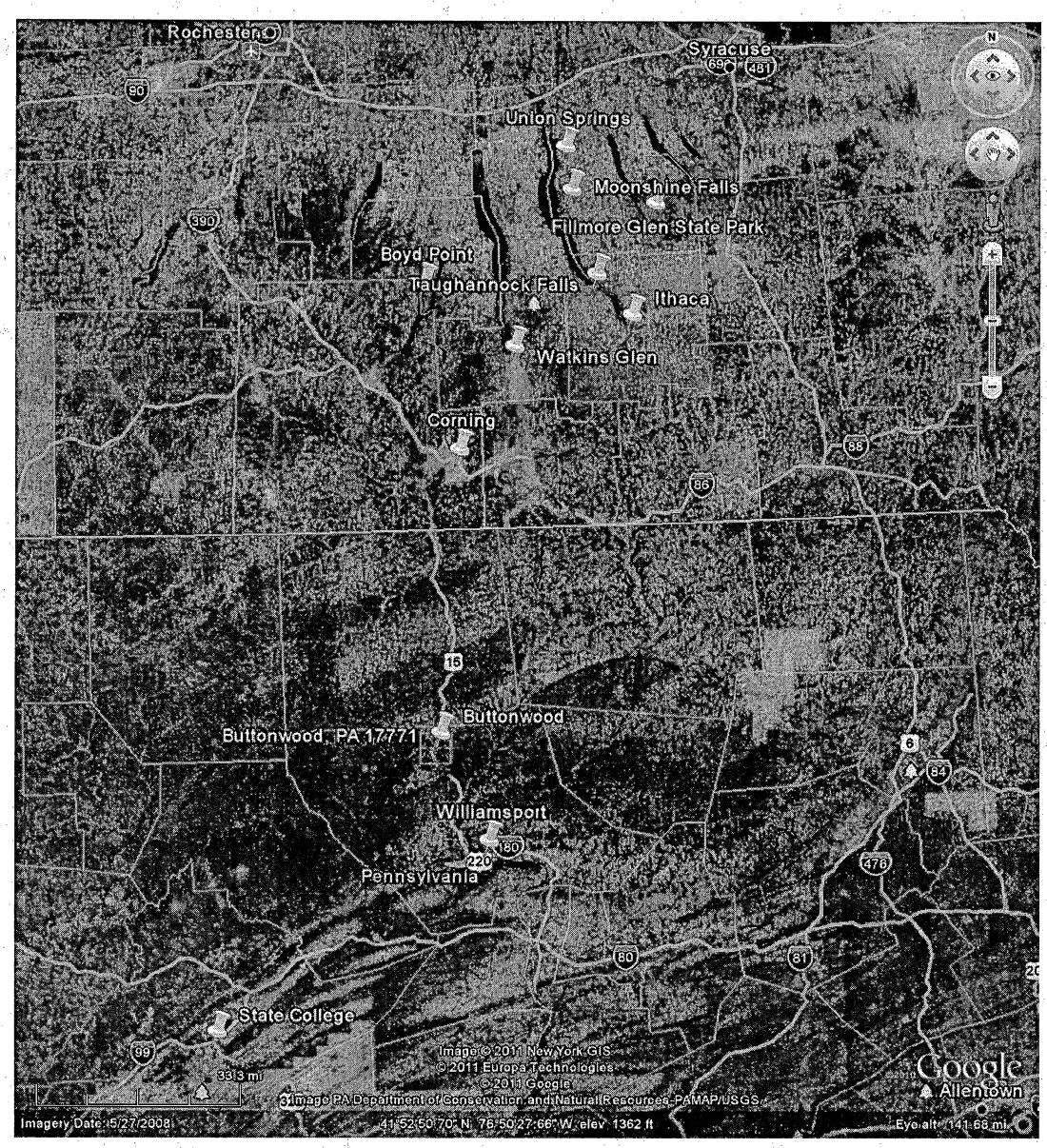

Figure 23. Map of outcrop locations examined during the June 2-3 field trip. Mapped with GoogleEarth.

Summary of findings

Key observations in outcrop are that there is a consistent fracture organization in terms of orientation and relative timing. Consistencies are seen across the outcrop belt and vertically through the section, with repeated patterns of fracture intensity in black and grey shales. These are summarized by Engelder and Gold (2008) field guide, in which some "conundrums" concerning our understanding of these fracture systems are discussed, and by Engelder et al. (2009). There are three main fracture sets: J1 joints,

trending ENE-WSW and best developed in the black shales such as the Marcellus, Geneseo and Middlesex Formations; J2 joints, trending approximately NNW-SSE, normal to fold axes and best developed in the grey shales; J3 which are sub-parallel to J1 but which tend to be curviplanar and are interpreted to have developed during uplift in the modern day stress field.

Fractures in outcrop mostly manifest themselves as barren joints with clear surface-propagation features such as plumose structure and arrest marks. Lacazette and Engelder (1992) documented an example in the Ithaca Sandstone and there are many other examples throughout the section (e.g. Fig. 24).

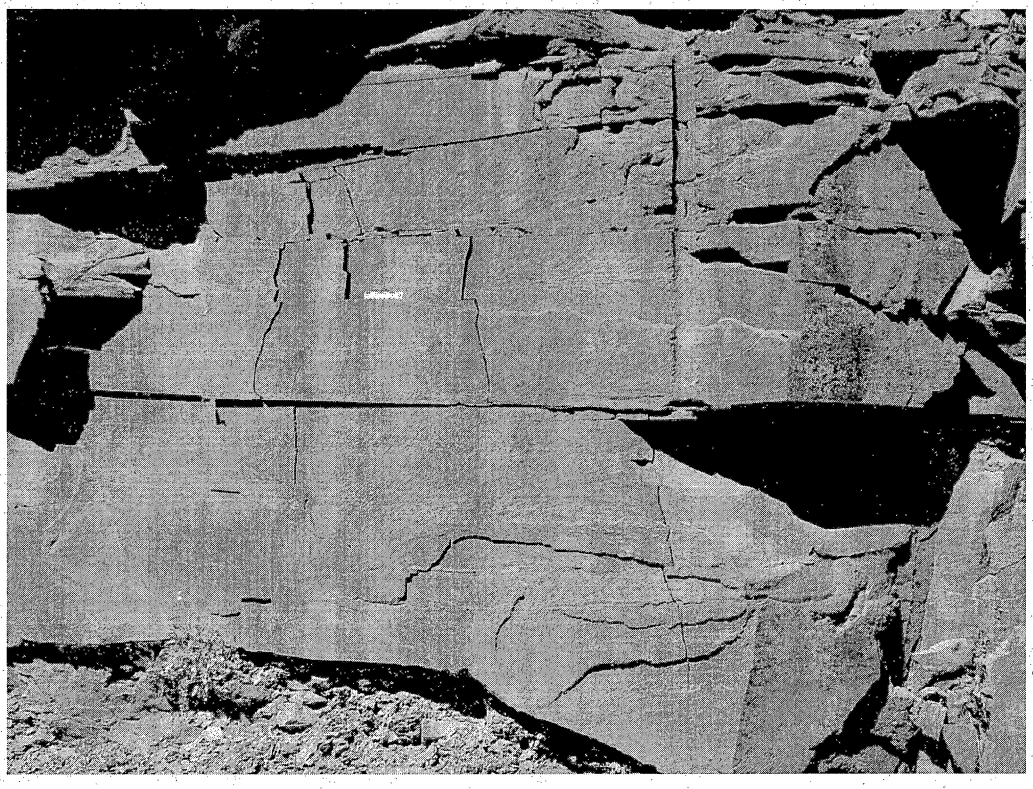

Figure 24. J2 joint with plumose structure showing several different horizons where fracture growth initiated. Catskill Delta Sherman Creek Formation sandstone south of Buttonwood on west side of I99.

J1 fractures are best developed in the black shale, and J2 are dominant in the grey shales. Both J1 and J2 occur in the grey shales directly overlying black shales (Fig. 25). There are in fact two sets of J2 joints, with the later set striking a little clockwise from the earlier set. At the Boyd Point stream outcrop the later J2 set are oriented 008/78 E (Fig. 26) and both J2 sets are also present at Taughannock Falls State Park, NY. (Fig. 27).

Figure 25. Both joint sets are present in Middlesex Shale in the streambed at Boyd Point, Keuka Lake, NY. A J2 joint is parallel to the scale (oriented (343/89NE here) and is at a high angle to J1 joints (oriented 077/90), which are offset along J2 joints in some places.

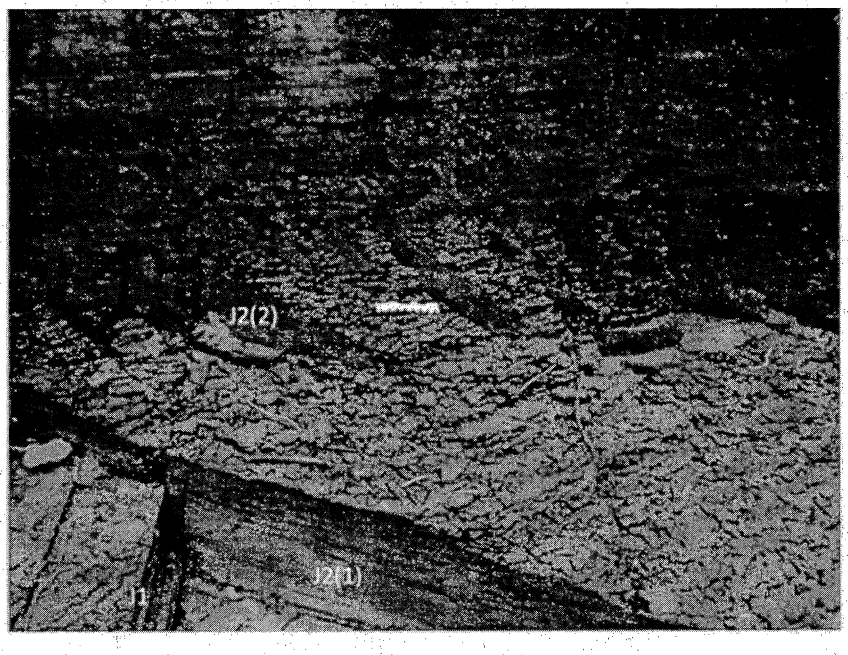

Figure 26. J1 and both J2 joint sets are present in the streambed at Boyd Point, Keuka Lake, NY.

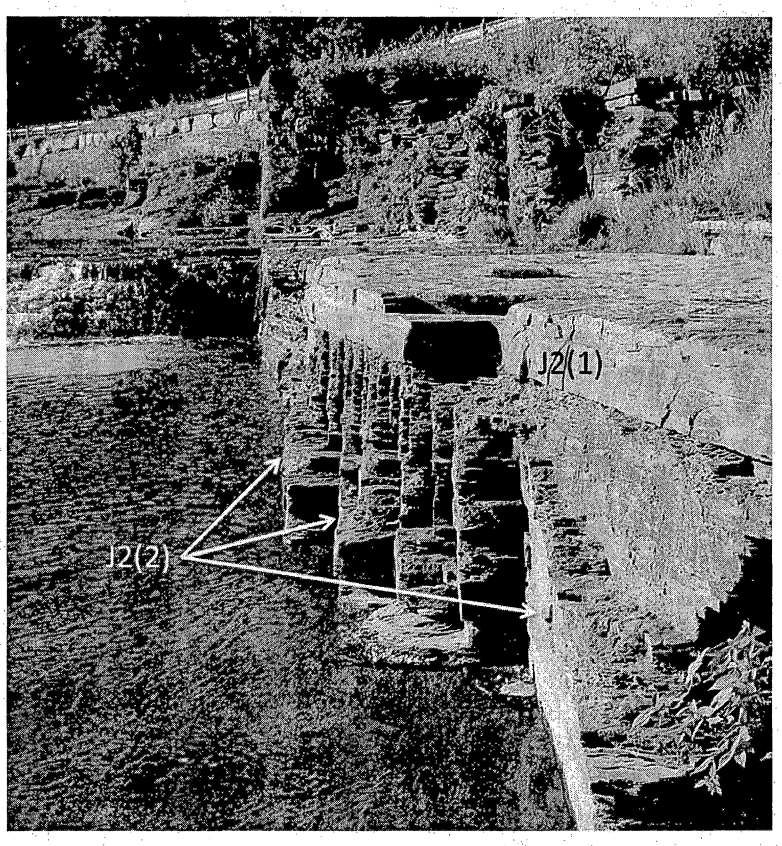

Figure 27. J2 joint sets, J2(1) and J2(2), are present in the Ithaca Formation at Taughannock Falls State Park, NY. Multiple J2(2) joints propagate down from the siltstone shale interface (Engelder and Gold, 2008).

Very few fractures have cement in them although there are exceptions (Fig. 28). A quarry near Union Springs, NY contains several well-exposed J1 joint surfaces with calcite and pyrite cement in the Union Springs Member of the Marcellus (J2 fractures also have cement). Further examples of cemented J2 joints are documented by Engelder and Gold (2008) in the Union Springs Member of the Marcellus along the Conrail railroad cut at Newton-Hamilton, PA. Partly open J2 fractures also occur in the Onondaga Limestone at the same location.

There are two sets with abutting and offset relations indicating an older J1 set that trends ENE-WSW and a younger J2 set trending NNW-SSE. Both are steeply dipping and sealed with calcite and pyrite. Kinematic apertures of these fractures are up to 1 mm and the cement-wall rock bond is weak.

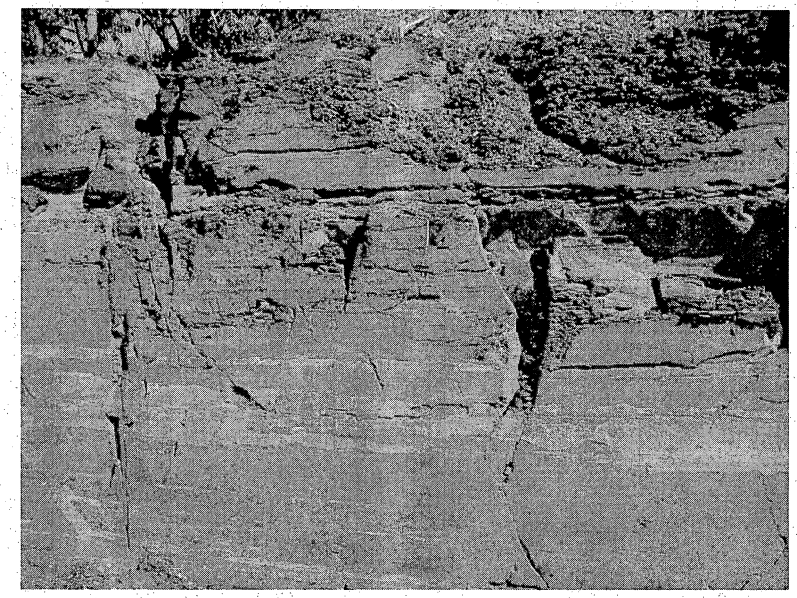

Figure 28. J1 fracture with calcite and pyrite cements on the surface. Plumose structure can be seen in the cement at right. Location: Wolfe Quarry, The Village at Union Springs, NY.

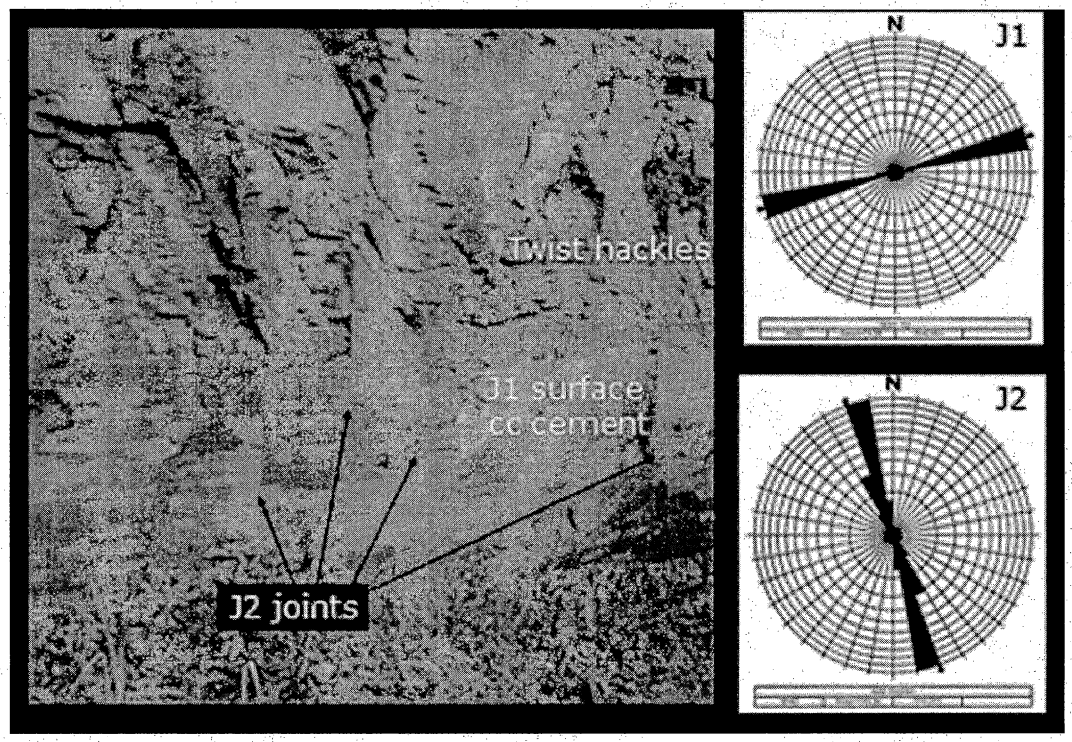

Figure 29. J1 fracture face with patchy calcite cement on the surface. Twist hackles have developed in the upper part of the fracture. Several J2 fractures cut the J1 fracture plane; J2 spacings, widths and other attributes were collected here using a scanline constructed along the J1 surface at approximately 1 m above the quarry floor. Inset rose diagrams; trends of J1 (n = 52) and J2 fractures (n = 42) measured at this location. Location: Wolfe Quarry, The Village at Union Springs, NY.

Natural fracture spatial organization.

Fracture spacing data were collected for both fracture sets. J1 spacing data were collected along a scanline normal to J2 fractures in the quarry floor. J2 data were collected along a scanline on a J1 joint surface that forms the back wall of the quarry (Fig. 29). Plots of fracture aperture versus position along scanline give a sense of the degree to which fractures are clustered. The J1 fractures are somewhat clustered (Fig. 30a), while the J2 fractures appear to be more strongly clustered (Fig. 30b). No mineral cement was seen in the J2 fractures in the scanline along the J1 that forms the back wall of the quarry although elsewhere in the quarry J2 fractures contain cement fill.

(a)

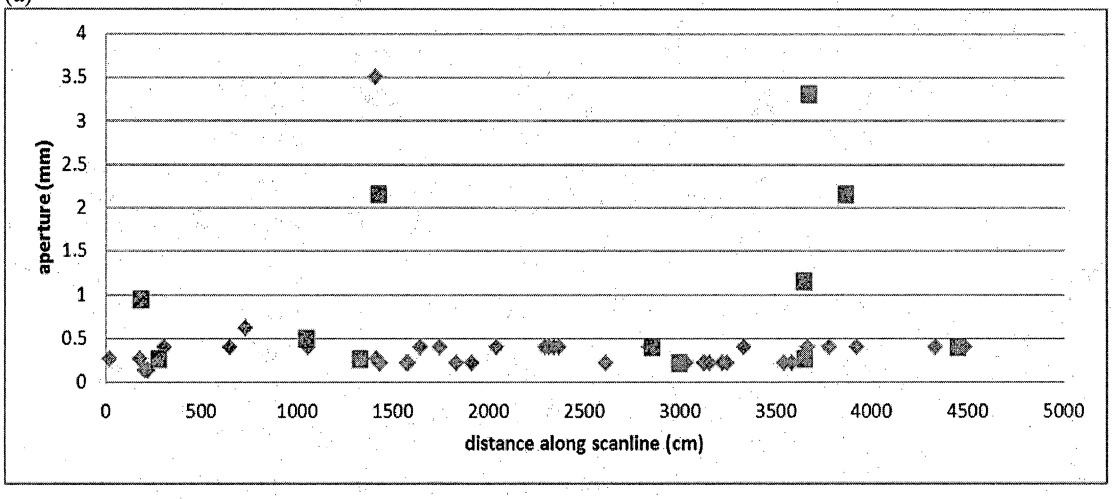

(b)

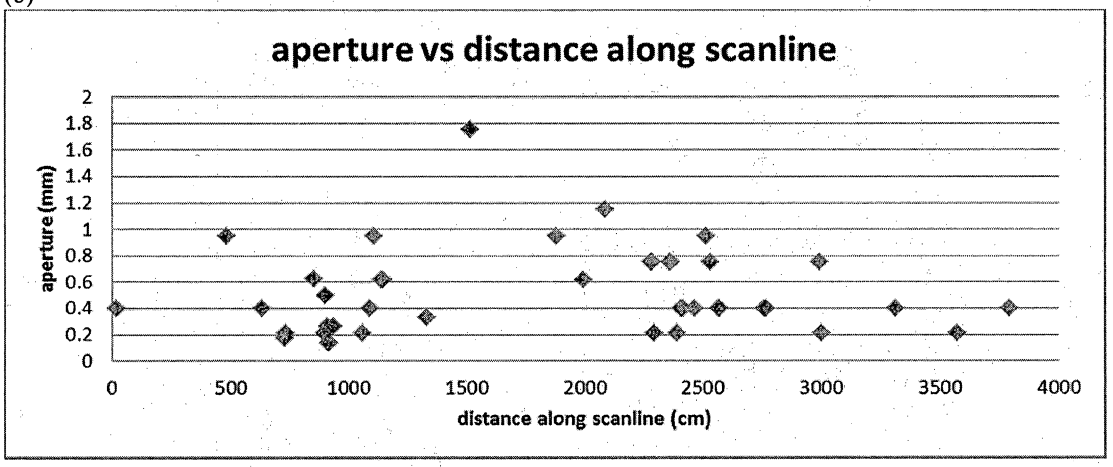

Figure 30. Plots of fracture aperture versus distance along scanline for (a) J1 joints, where orange = sealed fractures, blue = apparently barren fractures, and (b) J2 joints. Data were collected from scanlines normal to each joint set.

Plots of spacings, as shown in Figure 30, give a sense of clustering but do not allow quantification of clustering. To do this we analyzed the spacing data using a geostatistical method based on a two point correlation integral – the normalized correlation count (Fig.

31). This method, developed by Marrett et al. (2005) and Gomez (2007), allows quantification of the degree to which fractures are clustered relative to the clustering expected in a random distribution. The difference between the correlation count for a random set (normalized to 1) and the observed correlation count is termed the spatial correlation. Peaks in the observed data represent length scales at which spatial correlation is greater than random (Fig. 31). The J1 fractures have a weak preferred spacing at 0.2m, 1 m, ~7 m and 14 m (Fig. 31a). The J2 fractures show preferred spacing at 2, 4 and 14 m (Fig. 31b). The common correlation for both sets at 14 m is noteworthy and we speculate this may reflect an intrinsic mechanical layer thickness for the Union Springs at this location that persisted during burial and governed fracture spacing for two fracture sets that developed at two different times.

(a)

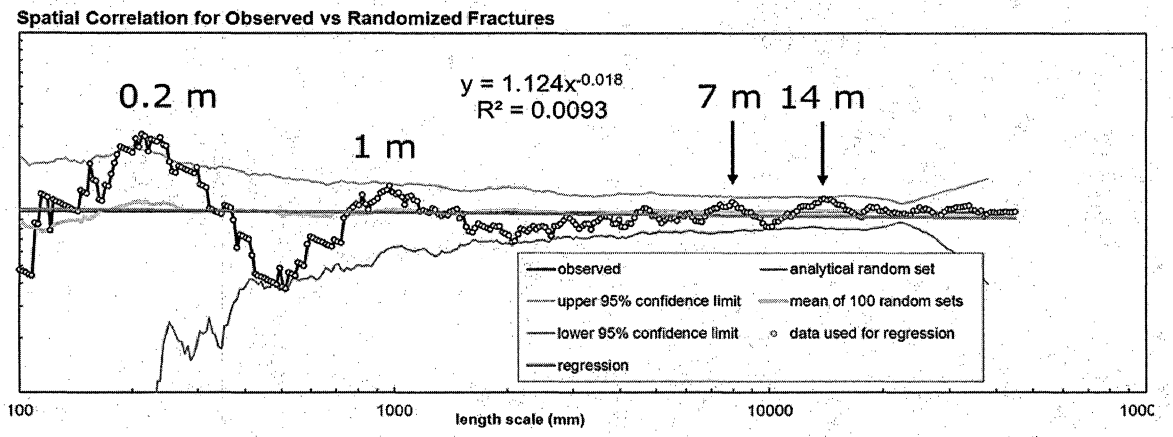

(b)

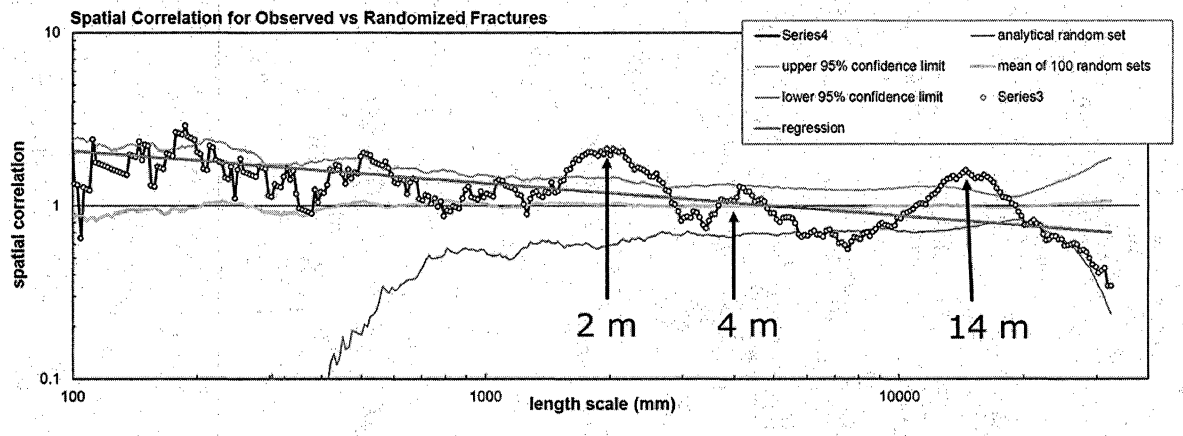

Figure 31. Spatial correlation plots for (a) J1 fractures and (b) J2 fractures in the Union Springs Member of the Marcellus Shale in the Wolfe Quarry at Union Springs, NY. Spacing data were collected along scanlines normal to each fracture set. The plots show the deviation of the observed data (open circles and black line) from analytical random spatial correlation (blue line) and 100 randomized arrangements of the data (green line) together with the 95% confidence limits of the randomized data. Peaks indicate greater spatial correlation at that length scale, troughs indicate lower correlation.

Natural fracture spatial organization: analysis of resistivity image log (GVR tool), Gulla Unit #10H Horizontal well, Washington Co., PA

The Gulla Unit #10H well in Washington Co. SW Pennsylvania is part of the group of five wells used in this project to characterize the natural fracture pattern in the Marcellus Shale. Of the five wells it is the only horizontal well. Fractures along the length of the wellbore, both natural and induced, were imaged with a Schlumberger GVR log, and bedding and fractures were interpreted and depths and orientations were plotted (picked) by Schlumberger. We extracted the fracture orientation data from an Excel spreadsheet of the fracture picks and plotted them as lower hemisphere stereographic projections (Fig. 32).

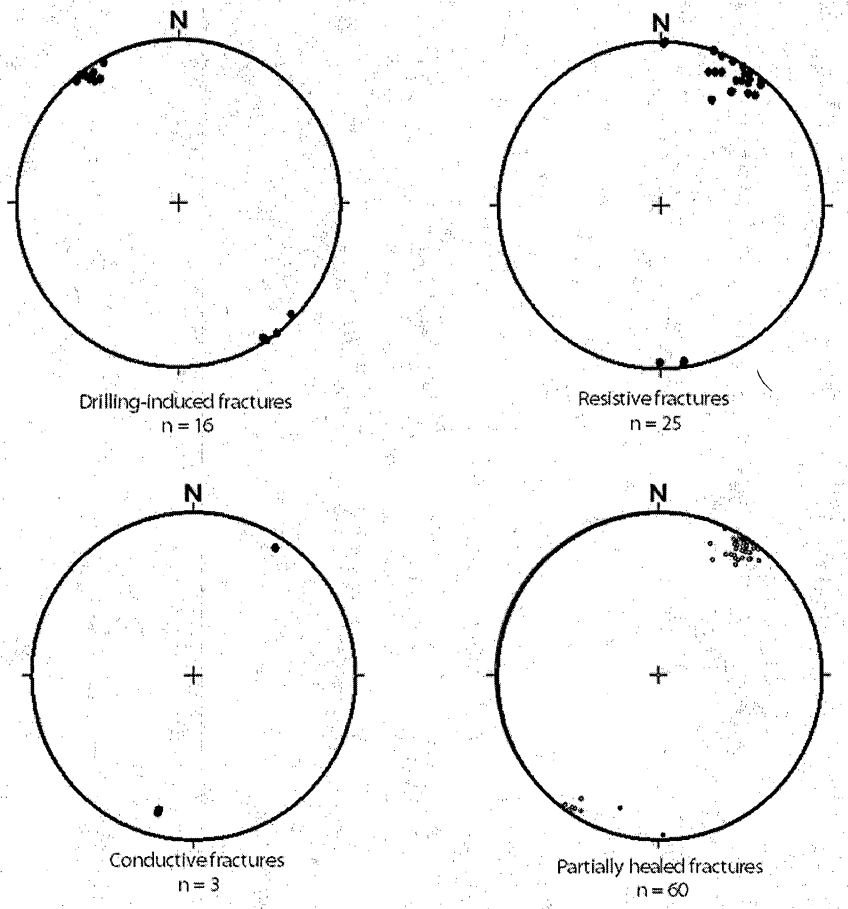

Figure 32. Compilation of lower hemisphere stereographic projections of poles to fractures for different fracture types identified in the Gulla Unit #10H image log. The drilling azimuth is 329°, which is normal to the drilling-induced fractures.

We also examined the fracture picks using the WellEye viewing tool and compared them with the fracture data obtained from core and image logs in the other wells in Washington Co. The orientations of different fracture types obtained from the image log in the Gulla Unit #10H well are similar to fracture orientations in the other wells at comparable depths. According to the directional survey the well becomes horizontal at about 6,366 ft (TVD) which corresponds to a MVD of 6,620 ft allowing for the curve around the heel of the well. This is close to the top of the Marcellus A.

Natural fractures with various degrees of resistivity trend WNW-ESE (these are interpreted as being part of the regional J2 set). Resistivity is an indicator of whether the fracture is open to conductive fluid. Conductive fractures are commonly interpreted as being open. Fractures with openings may have linings of cement on walls or may have been reactivated and opened during drilling. Partly open fractures may have discontinuous cement fill. Resistive fractures are likely to be filled with cement. The presence of all three degrees of mineral fill in a single set is consistent with models of cementation that show a size-dependence of fracture fill for synkinematic cement, or heterogeneity of fracture fill for postkinematic cements (Laubach 2003).

The orientation of fractures in this well and their measured depths along the length of the well allow us to examine the fracture spatial organization of the different fracture types. Examination of fracture occurrence along the length of the wellbore gives a qualitative sense of clustering (Fig. 33). Plots of fracture location along the borehole, from 6,660 to 7,208 ft (Fig. 33a) and from 7000 to 8364 ft (Fig. 33b) reveal the different fracture types are not evenly distributed. There are gaps in natural fracture occurrence between 6,800 and 7,000 ft and between 8,000 and 8,200 ft.

Drilling induced fractures trend NE-SW. It is possible some or all of the fractures interpreted as drilling induced are in fact natural J1 fractures. Otherwise, there are 88 J2 fractures, zero J1 fractures and 16 drilling-induced fractures in 1350 ft of lateral. Induced fractures (yellow in Fig. 33) are concentrated midway along the imaged borehole with a few at each end. The significance of this clustering of induced fractures (or J1) is not known at this point in the study. We will attempt to investigate further whether these fractures are natural or induced.

The deviation survey for the well indicates a drilling azimuth of 329°, which is normal to the induced fractures. An orientation sampling bias would lead to undersampling of WNW-ESE fractures more so than those trending at a high angle to the wellbore. We conclude that even if all the "induced fractures" are in fact J1 natural fractures, the J2 set is more intense than the J1 set at this locality.

(a)

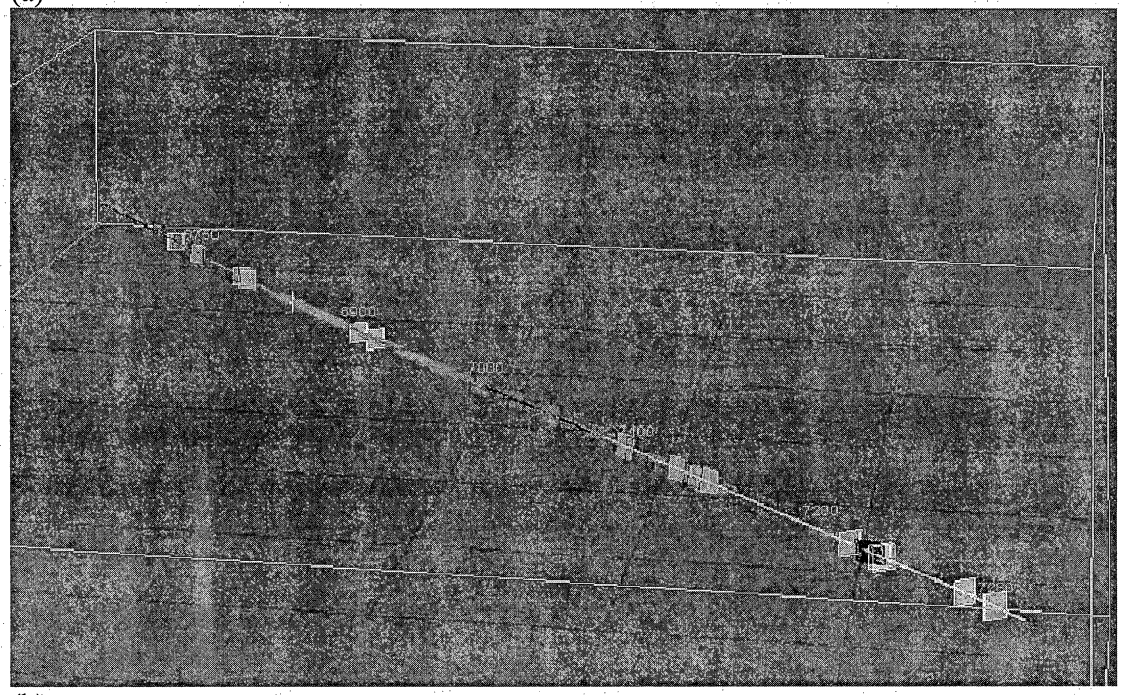

(b)

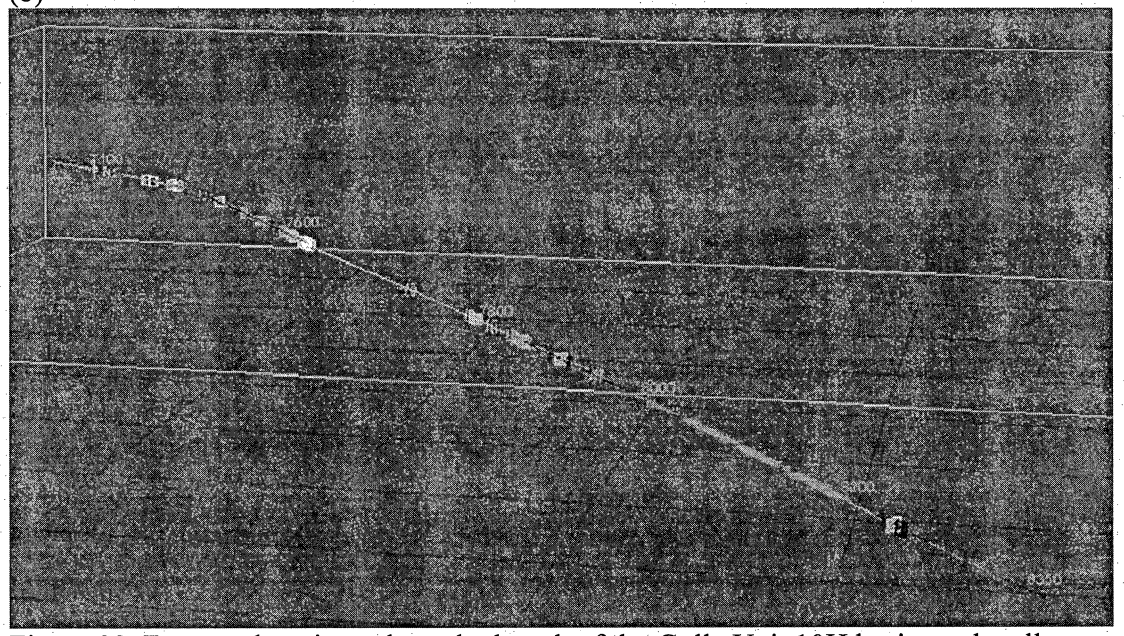

Figure 33. Fracture locations along the length of the Gulla Unit 10H horizontal well (picks by Schlumberger) (a)from 6,660 to 7,208 ft and (b) from 7000 to 8364 ft. Note overlap in the plots. Different fracture types are color coded: Red = partially healed fracture; Light blue = resistive fracture; Blue = conductive fracture; Yellow = drilling-induced fracture; Green = bed boundary.

The first step in our quantitative spatial analysis is to take the measured vertical depths along the wellbore and compute the spacings between all the fractures in the set. Corrections for non-oblique fractures can be made at this stage or after the correlation count analysis. The technique requires that the width (kinematic aperture, that is the wall to wall dimension of the fracture including porosity and cement) of the fractures be included so that mid-point positions for each fracture can be established. In the case of data collected in outcrop or horizontal core these would be directly measured, but because it is not possible to measure the widths of the fractures in the GVR log we assign arbitrary widths to the fractures. The widths are typical of those seen in core and range from 0.05 to 1 mm. A plot is made of the position of the fracture along the length of the wellbore, together with the assigned aperture size for each (Fig. 34). Comparison of the plot with the visualization of the wellbore for the drilling induced fracture shows how the plot captures the concentration of the fractures in the midsection of the well.

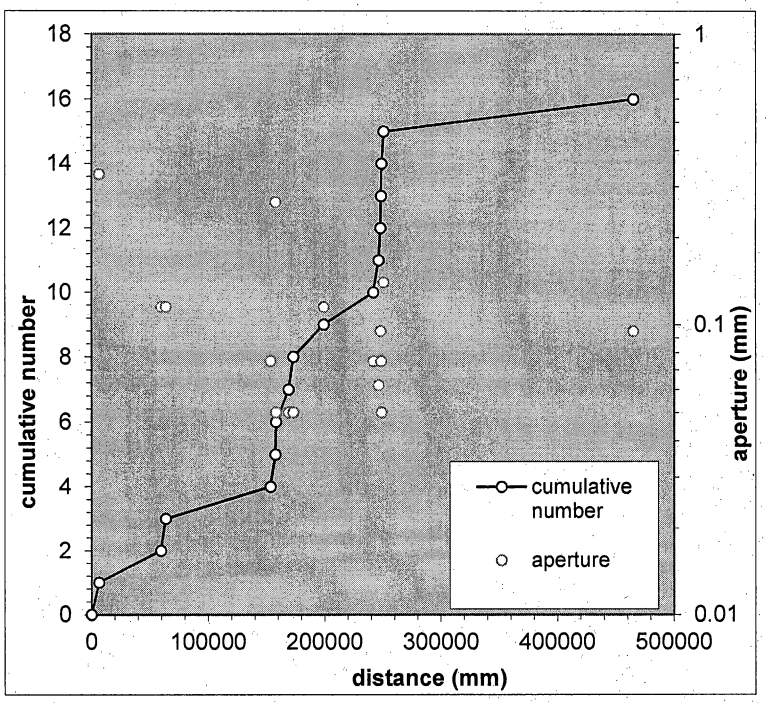

Figure 34. Plot of fracture location along the well bore (distance), shown as a cumulative fracture count (cumulative number). Widths (apertures) of each fracture are also shown. Drilling induced fractures.

We then use a modified correlation count technique, which is a geostatistical method based on a two point correlation integral. This method, developed by Marrett et al. (2005) and Gomez (2007), allows quantification of the degree to which fractures are clustered relative to the clustering expected in a random distribution. The difference between the correlation count for a random set (normalized to 1) and the observed correlation count is termed the spatial correlation (Fig. 35). Peaks in the observed data represent length scales at which spatial correlation is greater than random. In general, the larger the data set available the more representative it will be.

The plot for the drilling induced fractures shows a statistically significant peak around 80,000 mm (262 ft) (Fig. 35). This reflects the spacing of clusters of fractures seen around 170,000 and 250,000 mm in the plot of distance along borehole vs. cumulative number (Fig. 34) and in the yellow fractures in the borehole visualization close to marked depths of 7,280 and 7,500 ft (Fig. 33). Thus despite there being only 16 drilling induced fractures the correlation signal is high, indicating a strong spatial organization. The section of the plot from 1000 to 30,000 mm shows a spatial correlation progressively decreasing with increasing length scale. This is a mix of signal and artifact. The stepwise decrease with incremental decrease in length scale is due to the signal being obtained over progressively shorter distance as the length scale increases. However, the overall downward trend likely indicates a fractal spacing distribution within the clusters. Cluster width is approximately at the crossover on the x-axis at 16, 613 mm (55 ft)

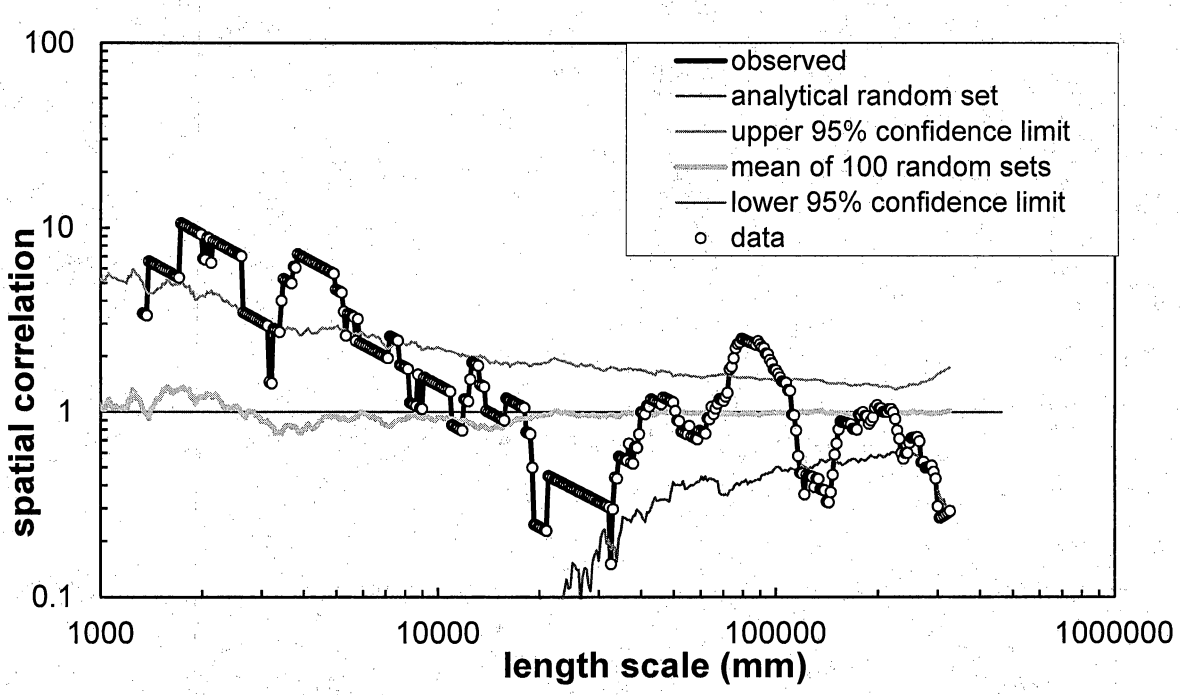

Figure 35. Spatial correlation plot for drilling induced fractures in the Gulla 10H well image log. The points up to 30,000 mm (~100 ft) indicate a fractal spacing distribution within clusters, while the peak at ~80,000 mm is an indication of a characteristic spacing, and it is statistically significant as it rises above the 95% confidence limit.

Although the natural fractures in the GVR log were split into three different groups on the basis of degree of mineral fill we argue above that these can be treated as a single set (J2). The combined data are plotted (Fig. 36) and analyzed (Fig. 37). In this case, in the absence of measured apertures, the apertures were assigned using a data set from an outcrop of Austin Chalk, where the largest fracture is 100 mm wide. These values are used to assign the midpoint of the fracture and have no further utility in this study. The cumulative number plot (Fig. 36) indicates the segments of the well bore along which there are many fractures (blue curve is steep) and those segments where there are no fractures (blue curve is flat).

The spatial correlation analysis (Fig. 37) shows a significant peak at 7,000, (23 ft) and weaker ones at 13,300 (44 ft) and 24,670 (81 ft). These all need to be corrected as the borehole is at a low angle to the fractures. If we take the mean trend of the fractures as 300° and the borehole direction as 329° then the correction to be applied is:
True spacing = apparent spacing (sin 29°)
Or, True spacing ≈ half apparent spacing
Thus the preferred spacings for J2 fractures are approximately at 3.5 m (11.5 ft), 6.75 m (22 ft) and 12.34 m (40 ft). The latter two are likely harmonics of the first. Unlike the plot for the induced fractures the natural fractures do not show a strong correlation at small length scales, progressively decreasing to zero or negative correlation. Rather, there is a single peak at 1500 -1700 mm (5 ft).

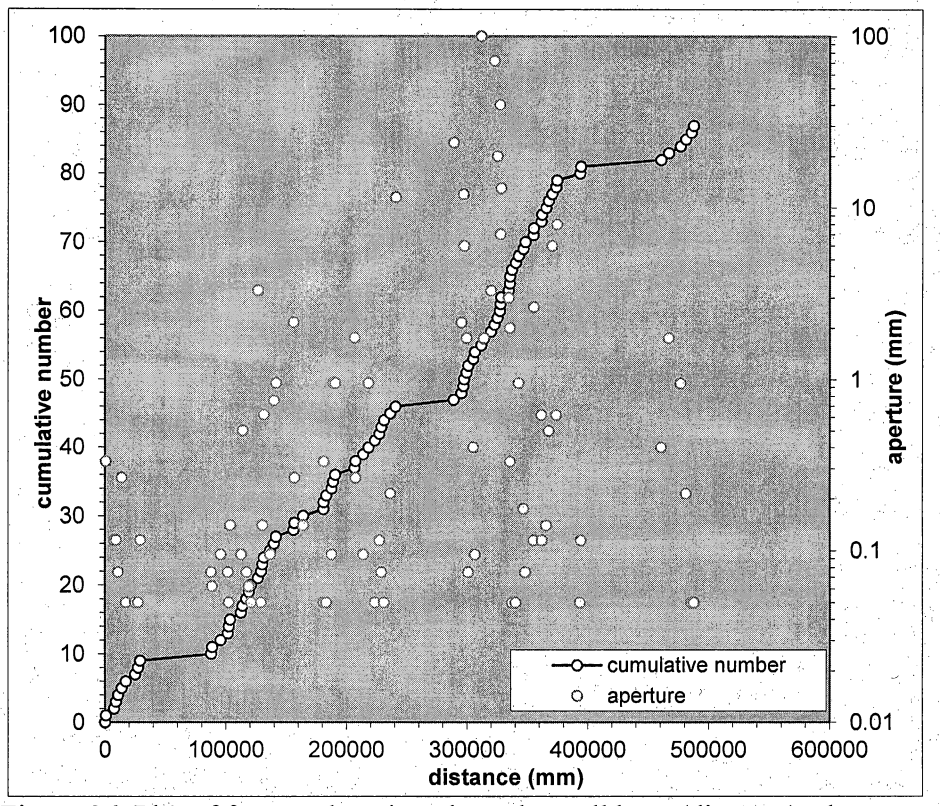

Figure 36. Plot of fracture location along the well bore (distance), shown as a cumulative fracture count (cumulative number) and fracture width (aperture) for natural fractures in the J2 set.

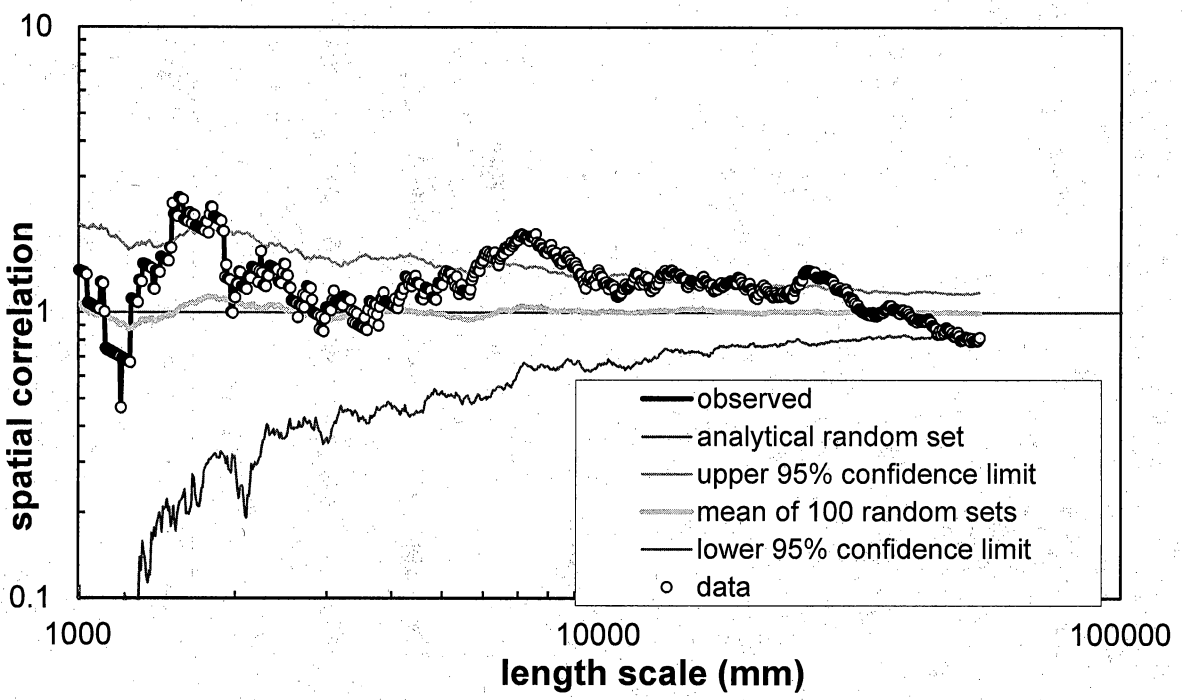

Figure 37. Spatial correlation plot for natural fractures in the Gulla 10H well image log. Significant spatial correlation is seen at approximately 1.5, 3.5, 6.8 and 12.3 m.

We now compare these results with fracture spacing data obtained from Marcellus Shale in a quarry at Union Springs, NY. In outcrop the J1 fractures have a weak preferred spacing at 0.2m, 1 m, ~7 m and 14 m. (These latter three spacings are not quite at the 95% confidence limit). The J2 fractures show preferred spacing at 2, 4 and 14 m. We highlighted the common correlation for both sets at 14 m in the field section of this report and speculated this may reflect an intrinsic mechanical layer thickness for the Union Springs at this location that persisted during burial and governed fracture spacing for two fracture sets that developed at two different times. The spacings for J2 obtained here are comparable to the spacings in outcrop. One would not expect a direct one to one correlation as the outcrop and reservoir are almost 300 miles apart and the actual spacings are sensitive to mechanical layer thickness. But the tendency to develop clusters and for these to be spaced perhaps 12-14 meters apart with some smaller scale clustering is common to both data sets. Inspection of the vertical pilot well logs for the Paxton Isaac well revealed thin limestone units at this 12.5 m spacing, and indeed we interpret the preferred spacing of fractures to reflect this mechanical layer thickness (Fig. 38). Spacings will modified by subcritical index also.

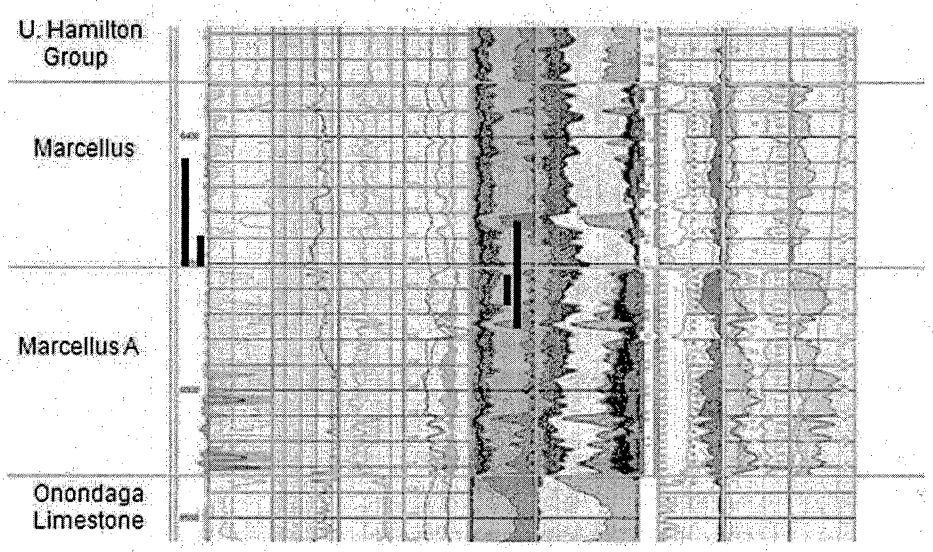

Figure 38. Paxton Isaac well log suite. The ECS shows limestone layers spaced at 12.5 m and 3 m. These may form boundaries to mechanical layers, which in turn control fracture height and thereby spacing.

The comparison with J1 is more problematic. If we assume all the "Induced fractures" are in fact J1 fractures that were reactivated during drilling there is still no similarity. In outcrop the J1 set were also clustered with clusters spaced weakly at around 14 m (with smaller spaced clusters within), but in the Gulla well these are spaced at 80 m. The difference could be due to the fact that the Gulla well samples a much longer distance normal to fracture strike than the outcrop. It is possible that our outcrop study contained just one large cluster of J1 as it was only about 45 m long.

Comparing empirically-derived spatial organization data with geomechanical modeling of fracture growth

The next phase of the spatial organization study was to compare the results from the outcrop and image log study with spatial analysis of fractures generated through geomechanical modeling of fracture growth. The modeling was done using JOINTS software, previously developed by Dr. Olson at The University of Texas at Austin. Modeling requires measurement of a mechanical rock property, the subcritical crack index (Holder et al., 2001). Measurements of subcritical crack index, fracture toughness and mechanical layer thickness from the Paxton Isaac well logs and samples were used as model input.

Geomechanical Testing

Core segments from the Paxton Isaac Unit #7 from Washington Co. (PI) and EGS#5 well (EG) from Lawrence County, were sampled for measurements of subcritical crack index (SCI) and Mode I fracture toughness (KIc, MPa-sqrt(m)). The reported Marcellus interval

in the EGS#5 well is 4010 to 4132 ft. The sample from 4082.2 ft yielded four test specimens, but the other samples (from 4099.4, 4106.7, 4119.2 and 4122 ft) could not be prepared because there was too little material for testing. SCI and K1c were determined from dual torsion measurements. The thicknesses of the test specimens are included in the tabulation. SCI was determined for 3 load decay measurements, followed by loading to failure (for K1c). Results are summarized in Tables 1 and 2.

Mean SCIs are 75, and 31, for the PI and EGS material. KIc values are generally 1 - 2 MPa-sqrt(m) for the Paxton Isaac samples and 0.7 MPa-sqrt (m) for the EGS#5.

Sample	Thickness	subcritical index					KIC
	(in)	1	2	3	4	5	Mpa-sqrt(m)
PI29S-4	0.084	78	95	92			0.36
PI29S-8	0.071	45	75	79			1.4
PI29S-9	0.075	65	80	88			1.4
PI85S-4	0.094	38	70	43			1.0
PI85S-6	0.082	67	73	57			1.2
PI85S-7	0.079	50	78	99			1.4
PI85S-8	0.075	81	123	131			2.2
PI85S-9	0.078	58	79	87			1.4
PI84S_A	0.080	76					1.3
PI84S_C	0.088			86			1.2
PI84S_D	0.085	60					1.7
PI84S_E	0.089	49					

Table 1. Subcritical crack index and fracture toughness results from tests on samples from the Paxton Isaac #7 well.

Sample	Thickness	subcritical index					KIC
	(in)	1	2	3	4	5	Mpa-sqrt(m)
EGSP4_1	0.075	27					
EGSP4_2	0.075	35					0.72
EGSP4_3	0.068	33	30				0.71

Table 2. Subcritical crack index and fracture toughness results from tests on samples from the EGS#5 well.

Geomechanical Modeling

In order to generate sufficient numbers of fractures to compare with outcrop and well datasets the output from the *JOINTS* geomechanical model was modified. The length of the model normal to fracture strike was extended while keeping the length parallel to fracture strike at least 5 times the layer thickness. We experimented with three different mechanical layer thicknesses: 1, 5 and 10 m. With this approach we were able to generate a model 200 m long so that a scanline constructed normal to the fractures intersected 39 fractures. This is comparable to the number of fractures observed in the field in 40 m scanlines and in the Gulla Unit #10H well. Spatial organization analyses of these different data sets are then compared.

We show a model using these input parameters and using a mechanical layer thickness of 10 m (Fig. 39). Although the fracture intensities are different and the number of fractures is low there are just sufficient (39) to give a signal in the spatial correlation plot (Fig. 40) so that spatial organization of these different data sets could be compared.

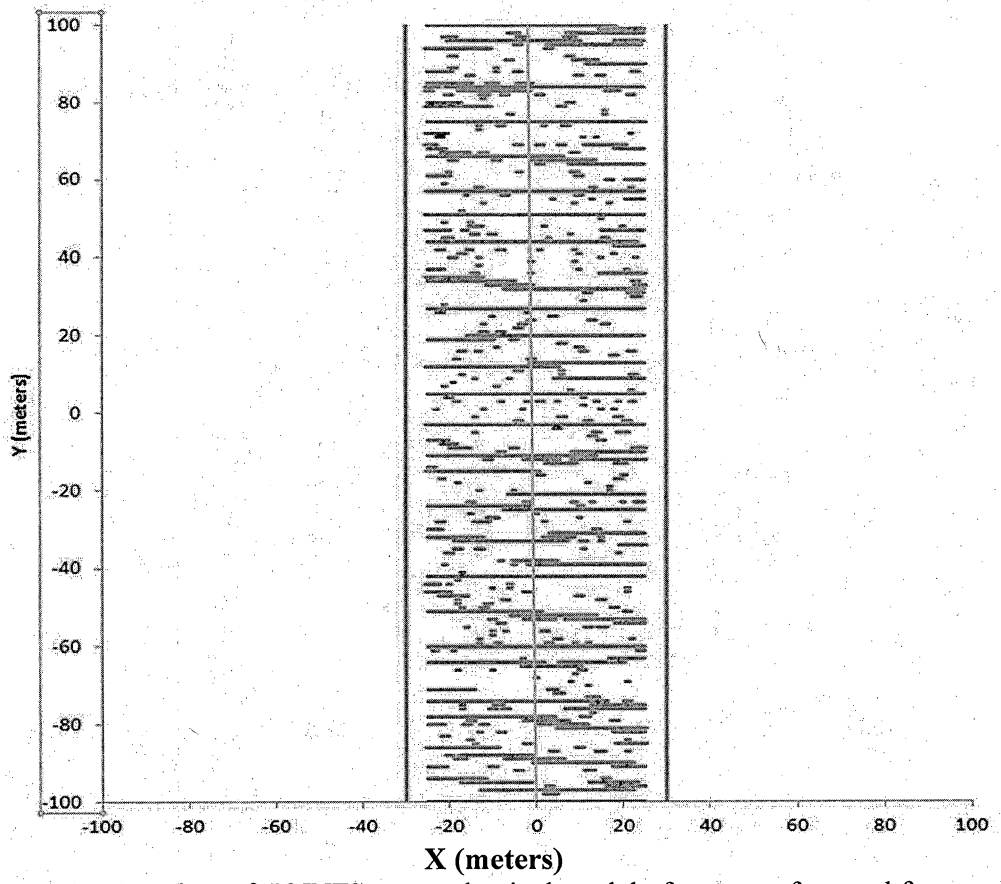

Figure 39. Map view of *JOINTS* geomechanical model of one set of natural fractures in Marcellus Shale using measured subcritical index (n= 80) and fracture toughness KIc = 1.3 MPa sqrm. Mechanical layer thickness is 10 m. Young's modulus and Poisson's ratio are chosen at 20 GPa and 0.2 respectively. Spacings and apertures were measured in the model along the orange line constructed normal to fractures at x = 0.

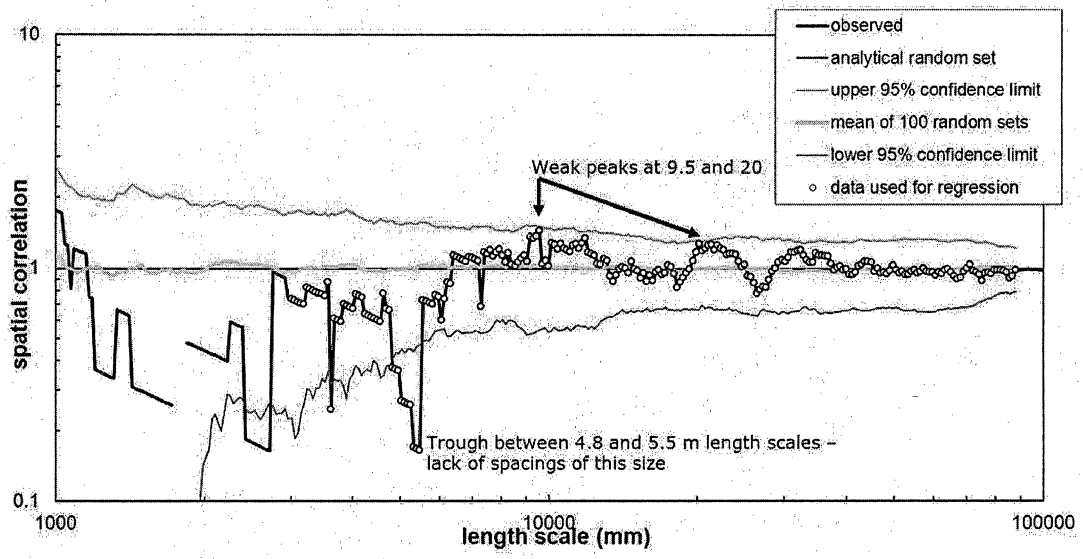

Figure 40. Spatial correlation plot for modeled fractures shown in Fig. 39.

Weak spatial correlation is seen at approximately 9.5 and 20 m. These correlation reflect the effect of mechanical layer thickness on fracture spacing. The subcritical index for this modeled example is 80, which is moderate to high and close to the mean for the sampels measured. Subcritical indices higher than this value would lead to more clustering of fractures, whereas indeices lower than 80 would lead to less clustering, but the mechanical layer thickness would still exert a strong control. The large trough between the 4.8 and 5.5 m length scale indicates lack of fracture spacings at this size.

Fracture Cement Studies: stable isotope work

Stable isotope work on some of the fracture cement samples expanded the original RPSEA project scope of work. Four samples of fracture calcite cement (2 outcrop from a quarry near Union Springs in that member, and 2 core samples from the Paxton Isaac well) were micro-drilled for analysis in a pilot study of $\delta^{13}C$ and $\delta^{18}O$ values. The samples from the outcrop J1 fractures show several narrow layers of calcite cement and a blocky cement section (Fig. 41). We interpret the layers as crack-seal texture, that is, repeated breaking and sealing of the fracture. The blocky cement is most commonly found in the fracture center but in some cases it is at the margin, which we interpret in terms of variation in the location of breaking from fracture to fracture. The J2 fracture we sampled has only blocky cement.

The fractures in the Paxton Isaac well sampled for the pilot study are both low angle, containing fibrous calcite cement fill (Fig. 42). We selected these as the most likely candidates to give a contrast in isotopic composition to the vertical sealed fractures from

the outcrop.

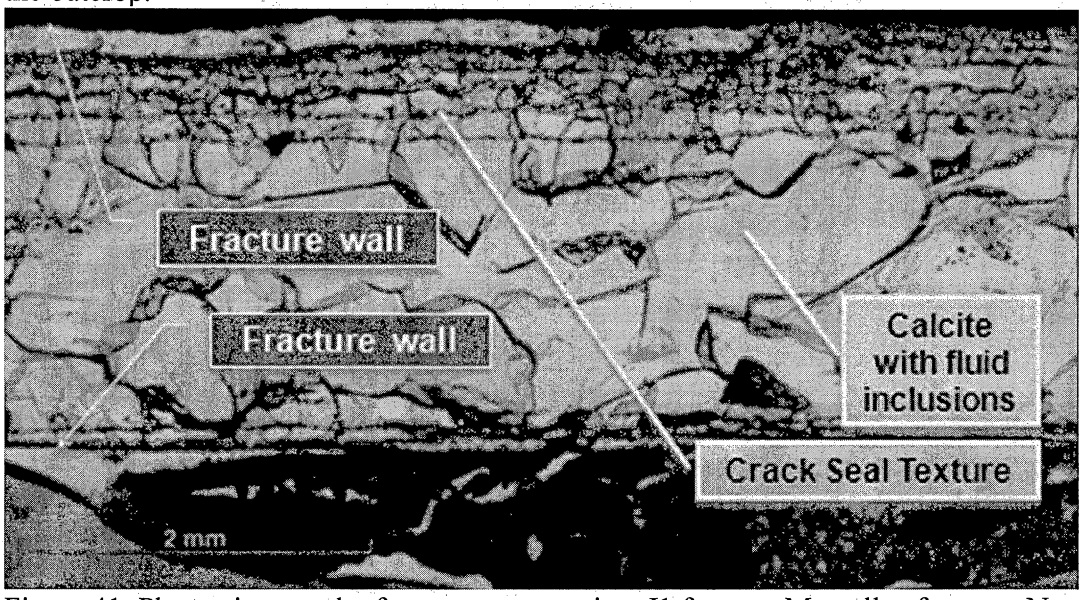

Figure 41. Photomicrograph of cement textures in a J1 fracture Marcellus fracture. Note the crack seal texture, delineated by of the presence of small, host rock inclusions parallel to fracture orientation. Blocky cement in the fracture center contains abundant fluid inclusions.

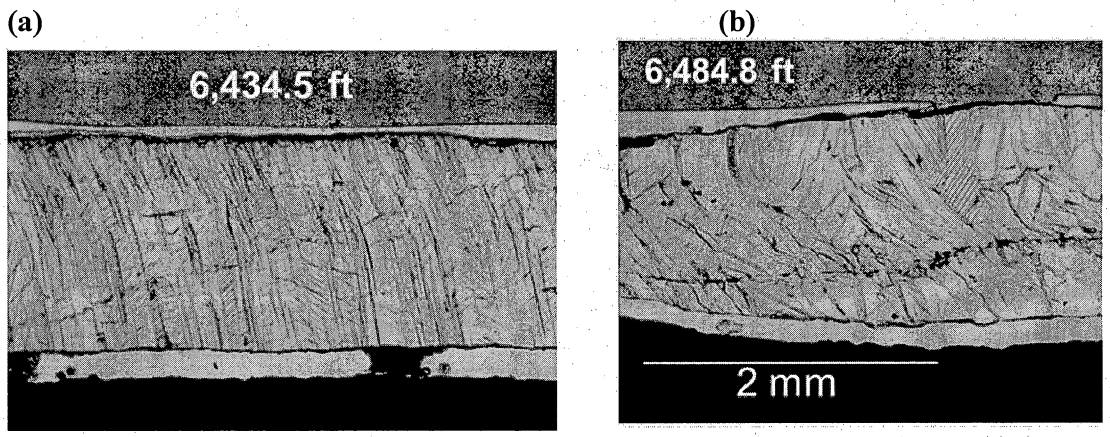

Figure 42. Fibrous calcite from horizontal and low angle fractures in the Paxton Isaac well. These samples were analyzed for $\delta^{13}C$ and $\delta^{18}O$.

The results of the stable isotope study are shown in Fig. 43. The samples from outcrop J1 and J2 have higher $\delta^{13}C$ and less negative $\delta^{18}O$ than those from the Paxton Isaac core (red circles). The interpretation of stable isotope data requires that temperature and growth rate effects be taken into account before concluding that source fluids are different. This study is outside the scope of the RPSEA project, but will be a major part of MS student Laura Pommer's thesis work. Pommer's thesis will be publicly available through the University of Texas at Austin library, and RPSEA funding will be acknowledged and the relation to the wider, GTI-led, Marcellus project will be made clear.

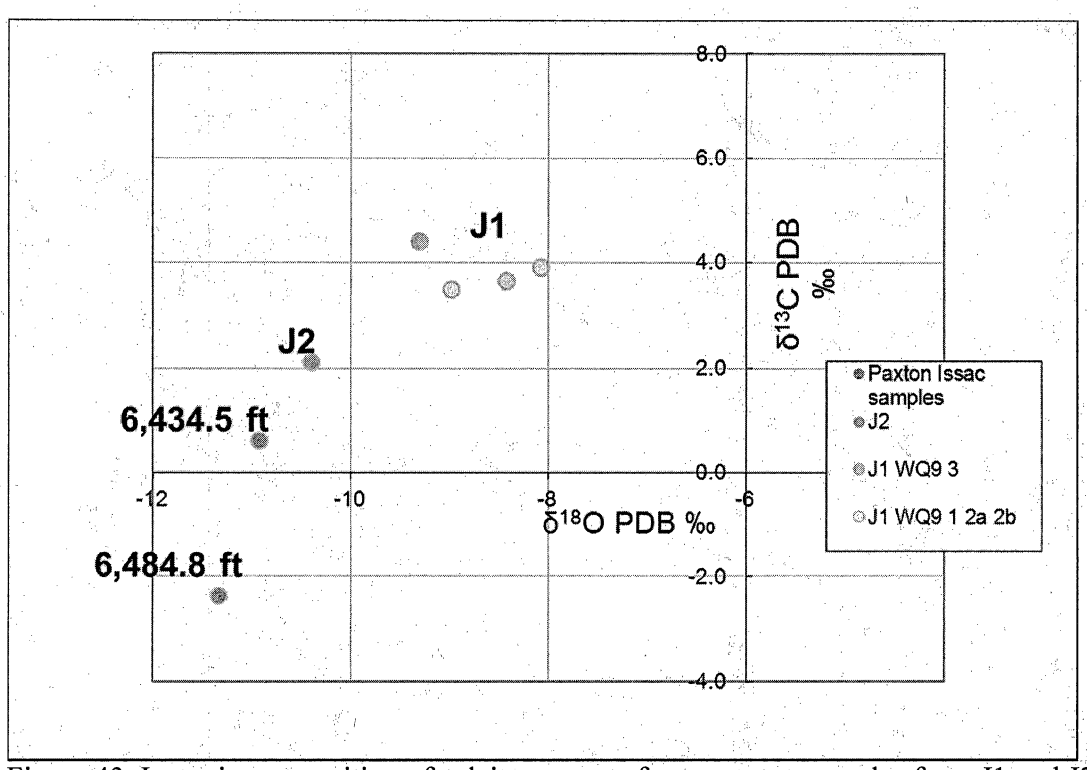

Figure 43. Isotopic composition of calcite cements from outcrop samples from J1 and J2 fractures in the quarry at Union Springs and core samples from the Paxton Isaac well.

Preliminary results.

For the purposes of this project the preliminary stable isotope results can be taken to indicate that there is potential in using stable isotope signatures of fracture cements to help distinguish fracture sets and sealing events in the Marcellus Shale. Fracture porosity and the strength of fracture planes are both dependent on the degree to which fractures are sealed so that knowledge of the sealing events is desirable.

Comparison of Fractures in Outcrop and Core

The striking difference between the outcrops and core is the degree of mineral fill observed. In core there are many filled fractures, whereas in outcrop most of the joint surfaces do not appear to have cement on them. There are exceptions, as noted above. An additional difference is that in core there are many examples of low-angle or horizontal filled fractures, but none were observed in the outcrops.

Technology Transfer

April 19-20th, 2011: Oral presentation (J.F.W. Gale) "Comparisons of natural fractures in the Marcellus Shale with fractures in other shale-gas plays. RPSEA Unconventional Gas Conference, Denver, Colorado.

September 25-27th 2011: Poster entitled "Natural Fracture Characterization in Shale-Gas Reservoirs: Spatial Organization and Fracture Sealing" presented at AAPG Eastern Section meeting, Arlington (Gale, Pommer and Ouyang).

September 28th 2011: Oral presentation (J.F.W. Gale) RPSEA Marcellus Workshop, Arlington.

October 31st, 2011: Guest lecture (J.F.W. Gale) on "Marcellus Shale Geology - Natural Fracture systems", Graduate Level Class "Advances in Unconventional Shale Gas Resources", University of Texas at Austin.

November 8th, 2011: Oral presentation (J.F.W. Gale) on "Marcellus Shale Geology - Natural Fracture systems" given to the Fracture Research and Application Consortium (FRAC) 2011 Sponsors' group meeting in Santa Barbara, CA. FRAC is an Industrial Associates program at The University of Texas at Austin.

February 20th-21st, 2012: J.F.W. Gale presented a poster at the Houston Geological Society Applied Geoscience Mudrocks Conference on "Natural Fracture Characterization in Shale-Gas Reservoirs: Spatial Organization and Fracture Sealing", where Marcellus examples from this project were included. The conference was attended by close to 400 people.

March 6th, 2012: J.F.W. Gale gave a talk on "Marcellus Shale Geology - Natural Fracture systems" at the Bureau of Economic Geology Mudrocks Industrial Associates sponsors' group meeting. The consortium has over 20 companies involved in North American and global mudrocks exploration and development.

March 31st, 2012: Laura Pommer presented her MS thesis work on "Fracture cementation in the Marcellus Shale" at The Jackson School of Geosciences Masters Saturday event, which was attended by students, faculty, industry sponsors and members of the public., Jackson School of Geosciences, The University of Texas at Austin.

April 17th, 2012: J.F.W. Gale oral presentation "Natural Fracture Attributes: Spatial Organization, Marcellus Gas Shale Project 09122-04" at the RPSEA Unconventional Gas Conference, Canonsburg, PA, 17-18th April, 2012.
April 24th, 2012: J.F.W. Gale and L. Pommer presented a poster on "Natural Fracture Characterization in Shale-Gas Reservoirs: Spatial Organization and Fracture Sealing" at the AAPG Annual Meeting in Long Beach, CA.

References

DOE Eastern Shale Gas Project reports (NETL website)

Engelder, T. and Engelder, R., 1977, Fossil distortion and décollement tectonics of the Appalachian Plateau, Geology, 5, 457-460.

Engelder, T. and Gold, D.P., 2008, Structural geology of the Marcellus and other Devonian gas shales: Geological conundrums involving joints, layer-parallel shortening strain, and the

contemporary tectonic stress field. Pittsburgh Association of Petroleum Geologists Field Trip (Sept. 12-13, 2008) AAPG-SEG Eastern Section Meeting Field Trip (Oct. 11-12, 2008).

Engelder , T., Lash, G.G. and Uzcategui, R.S., 2009, Joint sets that enhance production from Middle and Upper Devonian gas shales of the Appalachian Basin. AAPG Bulletin, v.93, p. 857-889.

Evans, M.A., 1980, Fractures in oriented Devonian shale cores from the Appalachian Basin: unpublished M.S. Thesis, Morgantown, West Virginia University, p. 278.

Evans, M.A., 1994, Joints and décollement zones in the Middle Devonian shales: Evidence for multiple deformation events in the central Appalachian Plateau: Geological Society of America Bulletin, v. 106, p. 447–460.

Evans, M. A., 1995, Fluid inclusion microthermometry: multiple vein sets from Middle Devonian shales GSA Bulletin, v. 107, p. 327–339.

Gale, J. F.W., 2002, Specifying lengths of horizontal wells in fractured reservoirs: Society of Petroleum Engineers Reservoir Evaluation and Engineering, Paper No. SPE 78600, p. 266–272.

Gale, J. F. W., and Holder, J., 2008, Natural fractures in the Barnett Shale: constraints on spatial organization and tensile strength with implications for hydraulic fracture treatment in shale-gas reservoirs, *In* 42nd U.S. Rock Mechanics Symposium and U.S.-Canada Rock Mechanics Symposium, San Francisco, June 29–July 2: ARMA, American Rock Mechanics Association, paper ARMA 08-96, 9 p.

Gale, J. F. W., and Holder, J., 2010, Natural fractures in some U.S. shales and their importance for gas production: The Geological Society, London, Petroleum Geology Conference Series, v. 7, p. 1131–1140.

Gale, J. F. W., and Laubach, S. E., 2010, New Albany shale fracture characterization: The University of Texas at Austin, Bureau of Economic Geology. Final report prepared for Research Partnership to Secure Energy in America (RPSEA), under GTI Contract Project No. S-48, 26 p.

Gale, J. F. W., S. E. Laubach, R. A. Marrett, J. E. Olson, J. Holder, and R. M. Reed, 2004, Predicting and characterizing fractures in dolostone reservoirs: Using the link between diagenesis and fracturing, *In* C. J. R. Braithwaite, G. Rizzi, and G. Darke, eds., The geometry and petrogenesis of dolomite hydrocarbon reservoirs: Geological Society (London) Special Publication 235, p. 177– 192.

Gale, J. F. W., Reed, R. M. and Holder, J., 2007. Natural fractures in the Barnett Shale and their importance for hydraulic fracture treatments. American Association of Petroleum Geologists Bulletin, 91, 603–622.

Gomez, L.A., 2007, Characterization of the Spatial Arrangement of Opening-Mode Fractures. Ph.D. Dissertation, UT Austin.

Harper, J., 2008, The Marcellus Shale—An Old "New" Gas Reservoir in Pennsylvania. Pennsylvania Geology, v. 38, no.1, Pennsylvania Bureau of Topographic and Geologic Survey.

Holder, J., J. E. Olson, and Z. Philip. 2001. Experimental determination of subcritical crack growth parameters in sedimentary rock. Geophysical Research Letters 28: 599–602.

Lacazette, A., and T. Engelder, 1992, Fluid-driven cyclic propagation of a joint in the Ithaca siltstone, Appalachian Basin,New York, in B. Evans and T.-F. Wong, eds., Fault mechanics and transport properties of rocks: London, Academic Press, p. 297–324.

Lash, G. G. and Engelder, T. 2005. An analysis of horizontal microcracking during catagenesis: example from the Catskill delta complex. American Association of Petroleum Geologists Bulletin, 89, 1433–1449.

Lash, G.G., and Engelder, T., 2007, Jointing within the outer arc of a forebulge at the onset of the Alleghanian Orogeny: Journal of Structural Geology, v. 29, p. 774–786.

Lash, G., and Engelder, T. 2009, Tracking the burial and tectonic history of Devonian shale of the Appalachian Basin by analysis of joint intersection style. Geological Society of America Bulletin, v. 121 p. 265 – 277.

Laubach, S. E., 1997, A method to detect natural fracture strike in sandstones: AAPG Bulletin, v. 81, p.604– 623.

Laubach, S. E., 2003, Practical approaches to identifying sealed and open fractures: AAPG Bulletin, v. 87, no. 4, p. 561–579.

Laubach, S.E., Olson, J.E., and Gale, J.F.W., 2004, Are open fractures necessarily aligned with maximum horizontal stress? Earth & Planetary Science Letters, v. 222, no. 1, 191-195.

Marrett, R., O. Ortega, and C. Kelsey, 1999, Extent of power-law scaling for natural fractures in rock: Geology, v. 27, no. 9, p. 799– 802.

Marrett, R.A., Gale, J.F.W. and Gomez, L.A., 2005, Spatial Arrangement of Fractures III – Correlation Analyses. Unpublished report prepared for University of Texas Fracture Research and Application Consortium.

Olson, J. E., 2004, Predicting fracture swarms—The influence of subcritical crack growth and the crack-tip process zone on joint spacing in rock, in J. W. Cosgrove and T. Engelder, eds., The initiation, propagation, and arrest of joints and other fractures: Geological Society (London) Special Publication 231, p. 73–87.

Appendix A

Dunn Clingerman and Nancy Stewart core fracture descriptions

Dunn Clingerman fracture descriptions

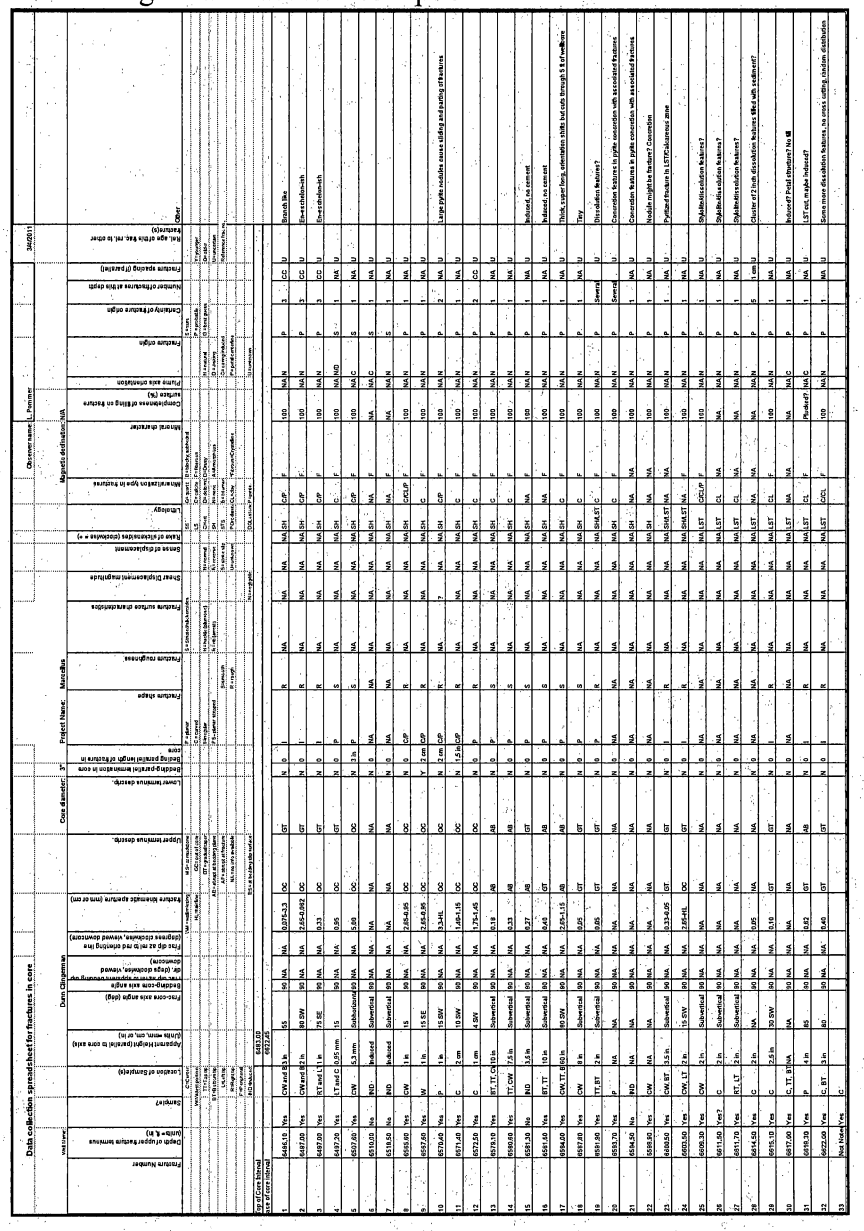

Nancy Stewart fracture descriptions

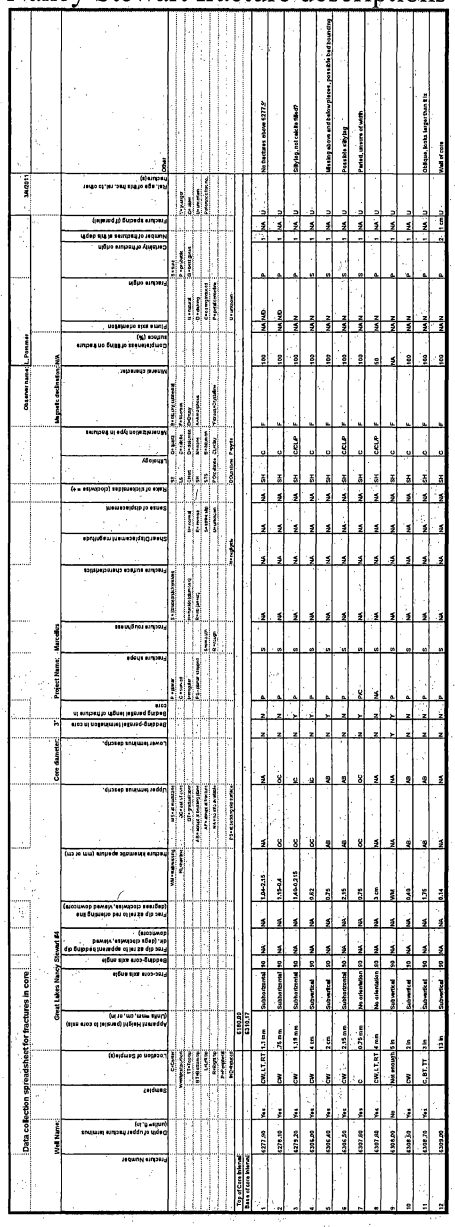

Appendix B

Sampling inventory for petrography and geomechanical tests. Samples labeled "double polished, standard thin sections with blue epoxy fill" were used for petrographic work, samples labeled "SCI" were used in geomechanical tests. Samples labled "gold coat" were to be analyzed with SEM for surface features, but this was not possible within the scope of the project.

Core samples from well experiment area

Sample	Sample type	Core Number-Terratek	Box Number-Terratek	Depth
PI 5909	2x3 Double polished, standard TS with blue epoxy fill	2	na	5909'
PI 5920.25	Bending test	2	na	5920' 2.5" -5920'7"
PI 5921.8	Double polished, standard TS with blue epoxy fill	2	na	5921' 8" - 5922'
PI 6231.5	Double polished, standard TS with blue epoxy fill	8	na	6231' 6" - 6232' 1"
PI 6382.1	Double polished, standard TS with blue epoxy fill	11	na	6382' 1" - 6382' 4"
PI 6384.8	SCI	11	na	6384' 8" - 6385'
PI 6429	SCI	12	na	6428' 10" - 6429' 3"
PI 6434.5	Double polished, standard TS with blue epoxy fill	12	na	6434' 5.5" - 6434' 11"
PI 6463	Double polished, standard TS with blue epoxy fill	12	na	6462' 7" - 6463' 3"
PI 6474	Double polished, standard TS with blue epoxy fill	12	na	6474' - 6474' 8"
PI 6484.5	Double polished, standard TS with blue epoxy fill AND GOLD COAT	13	na	6484.5' - 6484' 8"
PI 6484.8	Double polished, standard TS with blue epoxy fill	13	na	6484' 8"- 6485' 7"
H 7667.4	Gold coat	1	2	7667' 4' - 7668' 1"
H 7683	Double polished, standard TS with blue epoxy fill	1	8	7682' 11" - 7683' 3"
H 7691.4	Double polished, standard TS with blue epoxy fill	1	11	7691' 4" - 7691' 7"
H 7795.9	Double polished, standard TS with blue epoxy fill	3	5	7795' 11 " - 7796' 6"
H 7802.7	Double polished, standard TS with blue epoxy fill	3	7	7802' 7" - 7802' 11"
H 7827.2	Double polished, standard TS with blue epoxy fill	3	16	7827' 2" - 7827' 5"
H 7831.5	Gold coat	3	18	7831' 5" - 7832' 2"
H 7836.4a	Double polished, standard TS with blue epoxy fill	3	18	7836' 4" - 7838' 6"
H 7836.4b	Double polished, standard TS with blue epoxy fill	3	18	7836' 4" - 7838' 6"
H 7836.4c	Double polished, standard TS with blue epoxy fill	3	18	7836' 4" - 7838' 6"
H 7861	Double polished, standard TS with blue epoxy fill AND GOLD COAT	4	7	7861' - 7861'5"
H 7882.1	Double polished, standard TS with blue epoxy fill	5	3	7882' 1" - 7882' 11"
H 7889.25	Double polished, standard TS with blue epoxy fill	5	6	7889' 3" - 7890
H 7897.5	Double polished, standard TS with blue epoxy fill	5	8	7897' 6" - 7898' 1"
H 7899.6	Double polished, standard TS with blue epoxy fill	5	9	7899' 6" - 7900' 4.5"
H 7936	Double polished, standard TS with blue epoxy fill	6	2	7935' 11"- 7936' 1"
DC 6507.5	Double polished, standard TS with blue epoxy fill AND GOLD COAT	1	10	6507'6" - 6508'
DC 6570	Double polished, standard TS with blue epoxy fill	2	11	6570' - 6570'2"
DC 6572.2	Double polished, standard TS with blue epoxy fill	2	12	6572'3" - 6572' 6"
DC 6581.8	Double polished, standard TS with blue epoxy fill	2	15	6581'8" - 6582
DC 6592.1	Double polished, standard TS with blue epoxy fill	2	19	6592'1" - 6592'7"
DC 6593.5	Double polished, standard TS with blue epoxy fill	2	20	6593'6" - 6593'8"
DC 6600.5	Double polished, standard TS with blue epoxy fill	2	22	6600'6" - 6600' 10"
NS 6277.9	Double polished, standard TS with blue epoxy fill	3	16	6277'10" - 6278'6"
NS 6307.5	Double polished, standard TS with blue epoxy fill	4	4	6307'6" - 6308'

Field samples from quarry at Union Springs, NY

Sample	Sample type	Orientation Relative to Field Orientation	Notes
WQ1	Double polished, standard TS with blue epoxy fill	Horizontal	Horizontal relative to bedding for sampling vertical filled fracture J1
WQ2a	Double polished, standard TS with blue epoxy fill	Horizontal	Want caliche crust too if possible (on side)-Horizontal relative to bedding for sampling vertical filled fracture J1
WQ2b	Double polished, standard TS with blue epoxy fill	Horizontal	Horizontal relative to bedding for sampling vertical filled fracture J1
WQ3a	Double polished, standard TS with blue epoxy fill	Horizontal	Horizontal relative to bedding for sampling vertical filled fracture J1
WQ3b	Double polished, standard TS with blue epoxy fill	Horizontal	Horizontal relative to bedding for sampling vertical filled fracture J1
WQ4	Double polished, standard TS with blue epoxy fill	Horizontal	Horizontal relative to bedding for sampling vertical filled fracture J1
WQ5	Double polished, standard TS with blue epoxy fill	Mixed/Horizontal	Cement collection lined up parallel and cut across bottom
WQ6	Double polished, standard TS with blue epoxy fill	Horizontal	Little cement-Horizontal relative to bedding for sampling vertical filled fracture J1
WQ7	Double polished, standard TS with blue epoxy fill	Horizontal	Little cement-Horizontal relative to bedding for sampling vertical filled fracture J1
WQ8a	Double polished, standard TS with blue epoxy fill	Horizontal	Little cement-Horizontal relative to bedding for sampling vertical filled fracture J1
WQ8b	Double polished, standard TS with blue epoxy fill	Horizontal	Little cement-Horizontal relative to bedding for sampling vertical filled fracture J1
WQ9	Double polished, standard TS with blue epoxy fill	Mixed/Horizontal	Cement collection lined up parallel and cut across bottom
WQ10	Double polished, standard TS with blue epoxy fill	Mixed/Horizontal	Cement collection lined up parallel and cut across bottom
WQ11	Double polished, standard TS with blue epoxy fill	Mixed/Horizontal	Cement collection lined up parallel and cut across bottom